JACS
JOURNAL OF THE AMERICAN CHEMICAL SOCIETY
pubs.acs.org/JACS
Article

Strongly Polarized Iridium$^{\delta-}$–Aluminum$^{\delta+}$ Pairs: Unconventional Reactivity Patterns Including CO_2 Cooperative Reductive Cleavage

Léon Escomel, Iker Del Rosal, Laurent Maron, Erwann Jeanneau, Laurent Veyre, Chloé Thieuleux, and Clément Camp*

Cite This: https://doi.org/10.1021/jacs.1c01725
Read Online
ACCESS | Metrics & More | Article Recommendations | Supporting Information

ABSTRACT: The iridium tetrahydride complex Cp*IrH_4 reacts with a range of isobutylaluminum derivatives of general formula $Al(iBu)_x(OAr)_{3-x}$ (x = 1, 2) to give the unusual iridium aluminum species [Cp*$IrH_3Al(^iBu)(OAr)$] (**1**) via a reductive elimination route. The Lewis acidity of the Al atom in complex **1** is confirmed by the coordination of pyridine, leading to the adduct [Cp*$IrH_3Al(^iBu)$-(OAr)(Py)] (**2**). Spectroscopic, crystallographic, and computational data support the description of these heterobimetallic complexes **1** and **2** as featuring strongly polarized $Al(III)^{\delta+}$–$Ir(III)^{\delta-}$ interactions. Reactivity studies demonstrate that the binding of a Lewis base to Al does not quench the reactivity of the Ir–Al motif and that both species **1** and **2** promote the cooperative reductive cleavage of a range of heteroallenes. Specifically, complex **2** promotes the decarbonylation of CO_2 and AdNCO, leading to CO (trapped as Cp*IrH_2(CO)) and the alkylaluminum oxo ([$(iBu)(OAr)Al(Py)]_2(\mu$-O) (**3**)) and ureate ({$Al(OAr)(^iBu)[\kappa^2$-(N,O)AdNC(O)-NHAd]} (**4**)) species, respectively. The bridged amidinate species Cp*$IrH_2(\mu$-CyNC(H)NCy)$Al(^iBu)(OAr)$ (**5**) is formed in the reaction of **2** with dicyclohexylcarbodiimine. Mechanistic investigations via DFT support cooperative heterobimetallic bond activation processes.

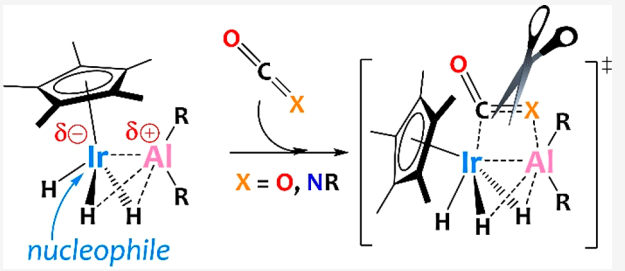

INTRODUCTION

Alkylaluminum(III) reagents are classically used in organometallic chemistry as catalysts activators—due to the propensity of these strong Lewis acids to perform halide or alkyl abstractions—leading to unsaturated, highly electrophilic transition-metal (TM) cations paired with weakly coordinating aluminate counteranions (Scheme 1, top). One of the most seminal applications of this chemistry is the widespread use of methylaluminoxanes (MAOs) as cocatalysts with metallocene complexes, which has revolutionized polyolefin synthesis.[1,2] In contrast, in this contribution, we describe a very rare example where alkylaluminum species promote umpolung at a d-block metal, converting iridium half-metallocenes into nucleophiles through the formation of polarized $Ir^{\delta-}$–$Al^{\delta+}$ pairs (Scheme 1, bottom).

The study of TM complexes bearing aluminum-based metallo-ligands is still in its infancy. This is mostly due to the synthetic challenges associated with the preparation of such heterobimetallic species in a controlled way, which requires the introduction of an Al center, the derivatives of most of which are Lewis acidic, in the coordination sphere of a TM, classically acting as a Lewis acids as well. Yet, such derivatives hold great promises in terms of reactivity. In the case of late transition metals, which feature higher electronegativities in comparison to Al (1.61 on the Pauling scale), the binding of hard Al-based ligands, acting as σ-acceptors, can reverse the classical ligand→TM bonding situation and confer unique electronic properties

Scheme 1. Contrasting Reactivity of Alkylaluminum Reagents with d-Block Metal Species

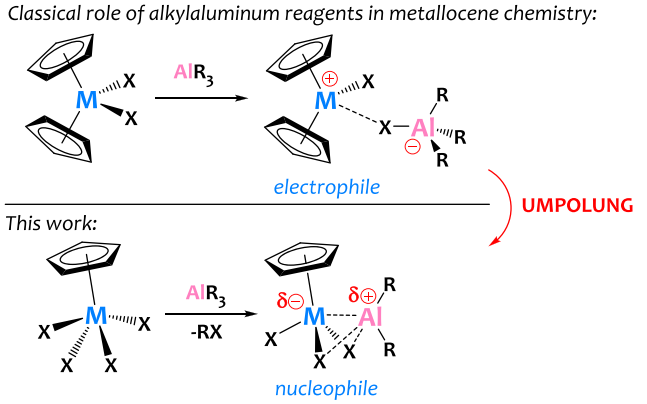

Received: February 12, 2021

to the resulting complexes, which opens up attractive opportunities for cooperative reactivity. Although a range of Z-type metal−alane $L_nM{-}AlX_3$ Lewis adducts are known,[3−13] complexes featuring X-type metal−aluminum $L_nM{-}AlX_2(L'_m)$ (m = 0, 1) covalent bonds are much more rare (Scheme 2) and their reactivity remains almost unexplored.[14−22]

Scheme 2. Representative Examples of Formally X Type Aluminum Ligands Bound to Late Transition Metals and Related Species of Relevance to the Current Study

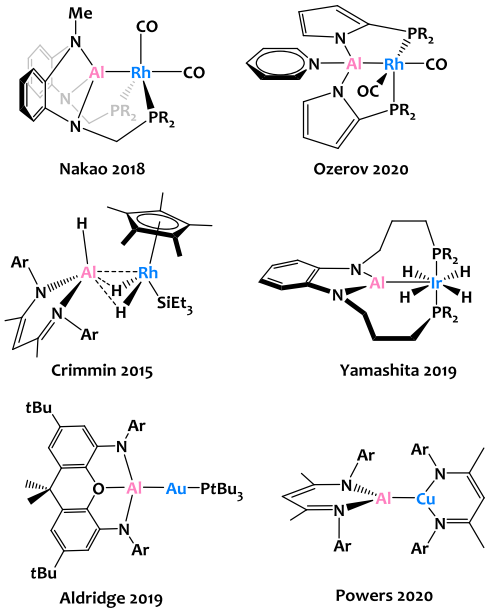

A groundbreaking achievement in this area was reported in 2019 by Goicoechea, Aldridge, and colleagues, who described the transfer of polarity between gold(I) and a "naked" (NON) Al aluminyl(I) anion, leading to an $Al^{\delta+}{-}Au^{\delta-}$ complex.[19] A direct consequence of this umpolung is the unusual nucleophilic reactivity at the gold center observed in the reductive insertion of CO_2. Very recently, Power reported the preparation of an aluminum−copper metal−metal-bonded species from Al(I), $(BDI^{Mes})CuAl(BDI^{Dip})$,[23] and Arnold reported rare examples of An−Al dative interactions (An = U, Th),[24,25] but the reactivity of these species was not described.

It is important to note that all of the reported late-metal−aluminum systems, shown in Scheme 2, rely on the use of electronegative amido α-substituents to stabilize the Al center. Although alkyl-substituted aluminyl anions and a monomeric alanediyl species have been synthesized very recently,[26−29] their coordination chemistry to late transition metals has yet to be demonstrated. One notable exception is the unusual ethylaluminum complex $[Cp^*(PMe_3)Ir(AlEt)]_2$ (Scheme 3, top), reported by Bergman and co-workers in 1998.[13] This compound was prepared without the requirement of isolating challenging low-valent Al−alkyl species, via a simple double deprotonation of a dihydride iridium(III) complex by the commercially available triethylaluminum reagent.[30] To our surprise, no followup studies emerged from this preliminary work to explore further the reactivity of this unconventional molecular object featuring a low-valent Ir_2Al_2 core. Very recently, our group reported the preparation of heterobimetallic tantalum−iridium complexes using a similar alkane

Scheme 3. Representative Reductive Alkane Elimination Reactivity of Pentamethylcyclopentadienyl Iridium Polyhydrides with Nucleophilic Metal−Alkyl Derivatives Reported in the Literature[13,31]

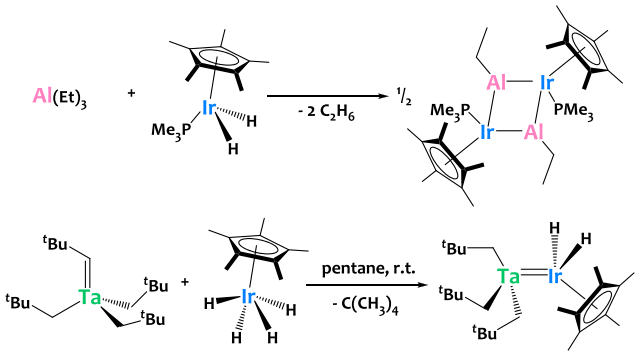

reductive elimination approach (Scheme 3, bottom) and demonstrated the ability of the resulting Ta═Ir multiple-bond motif to promote H/D isotope exchange reactions with excellent catalytic performances.[31−33]

Inspired by this exploratory work from Bergman and co-workers, and in a continuation of our previous work, we hypothesized that this alkane elimination chemistry could be extended to the preparation of well-defined iridium systems bearing aluminum-based ligands. Such an approach could open up unusual mechanistic pathways and help in an understanding of more complex chemistry, such as the multifaceted role of alkylaluminum reagents employed as cocatalysts in numerous transition-metal-catalyzed processes. Accordingly, we investigated the reactivity of aluminum isobutyl derivatives toward the iridium tetrahydride complex Cp^*IrH_4,[34] which led to the formation of unusual bimetallic complexes featuring strongly polarized $Al^{\delta+}{-}Ir^{\delta-}$ cores. These heterobimetallic complexes were notably able to reductively cleave heteroallenes (CO_2, isocyanates).

RESULTS AND DISCUSSION

Preparation of Bimetallic Ir/Al Species. In view of preventing the formation of tetrametallic aggregates such as those observed by Bergman[30] (Scheme 3), we considered the use of sterically hindered Al−alkyl sources. For that purpose, we employed bulky isobutylaluminum aryloxy precursors and explored their reactivity toward Cp^*IrH_4.

Treatment of diisobutyl(3,5-di-*tert*-butyl-4-hydroxytoluene)-aluminum, denoted $Al(^iBu)_2(OAr)$, with Cp^*IrH_4 results in the formation of the heterobimetallic complex $[Cp^*IrH_3Al(^iBu)(OAr)]$ (**1**) which is isolated in 72% yield after 24 h of reaction at room temperature (Scheme 4). One equivalent of

Scheme 4. Synthesis of the Al−Ir Heterobimetallic Species 1

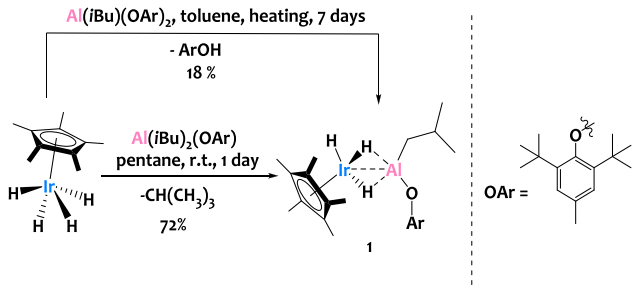

https://doi.org/10.1021/jacs.1c01725
J. Am. Chem. Soc. XXXX, XXX, XXX−XXX

isobutane (quantified by ^{1}H NMR, see Figure S1) is released in the course of the reaction. The ^{1}H NMR spectrum of **1**, recorded in C_6D_6 solution, shows isobutyl signals at δ 2.15, 1.08, and 0.31 ppm integrating respectively for 1H, 6H, and 2H and indicating the presence of one isobutyl group per Al center as expected. The hydride resonance is observed as a singlet at δ −16.80 ppm and integrates for 3H. This suggests rapid exchange among the three hydrides on the NMR time scale at room temperature, which is expected on the basis of literature precedents for metal−polyhydride systems.[32,33,35,36] The IR spectrum of **1** exhibits two strong bands at σ 2144 cm^{-1} and 1973 cm^{-1} assigned to metal−hydride stretches. The most significant feature of the crystallographic structure of **1**, shown in Figure 1, is the Al−Ir distance of 2.406(2) Å, which

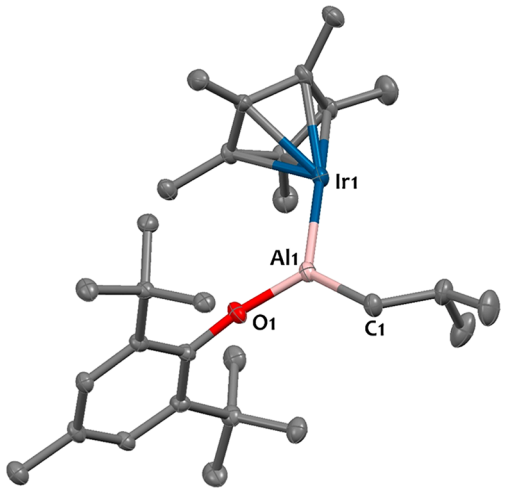

Figure 1. Solid-state molecular structure of **1**. Displacement ellipsoids are plotted at the 30% probability level. Hydrogen atoms have been omitted for clarity. Selected bond distances (Å) and angles (deg): Ir1−Al1 2.406(2), Al1−O1 1.695(4), Al1−C1 1.961(6), O1−Al1−Ir1 120.60(18), O1−Al1−C1 115.4(3), C1−Al1−Ir1 124.0(2). Al1−Ir1−Cp*$_{centroid}$ 143.8(2).

is the second shortest reported distance for a Ir species bearing an Al atom in its coordination sphere.[30,37−39] The only species featuring a shorter Al−Ir bond of 2.382(1) Å is the pincer complex [PAlP]Ir(H)$_4$ (Scheme 2) described by Yamashita and co-workers.[16] The metal−metal separation in **1** is 0.10 Å shorter than the sum of the metallic radii of aluminum (1.248 Å) and iridium (1.260 Å),[40] which translates into a formal shortness ratio below unity (r = 0.959).[41] Therefore, although the close proximity between the Al and Ir centers in **1** is most likely the result of the presence of bridging hydrides, a direct metal−metal interaction cannot be excluded. Overall, this result suggests a strong donation of the Cp*IrH$_3$ iridate fragment onto the cationic Al(III) site. The high electrophilicity of the Al cation in **1** is also reflected in the short Al1−O1 bond of 1.695(4) Å in comparison to similar Al−O$_{Ar}$ parameters found in the literature.[42−44] Another characteristic of the structure of **1** is the marked tilting of the Cp* ring with respect to the Al−Ir axis (Al−Ir−Cp*$_{centroid}$ angle of 143.79°). We propose that this geometrical arrangement is due to the presence of a terminal hydride on the Ir center, as confirmed by computational data (see below).

In contrast to Al(^{i}Bu)$_2$(OAr), the more hindered species isobutylbis(3,5-di-*tert*-butyl-4-hydroxytoluene)aluminum, denoted Al(^{i}Bu)(OAr)$_2$, does not react with IrCp*H$_4$ in toluene at room temperature. Upon heating at 110 °C for 1 week, compound **2** is obtained from Al(^{i}Bu)(OAr)$_2$ and is isolated in 18% yield from cold (−40 °C) recrystallization in a saturated pentane solution (Scheme 4). ^{1}H NMR monitoring of this reaction indicates the release of 2,6-di-*tert*-butyl-4-methylphenol (see Figure S2). We attribute the preferential reductive elimination of HOAr versus isobutane to the particularly high steric hindrance of this phenoxy derivative. Note that complex **1** does not react with HOAr, even upon heating, while treatment of **1** with 1 equiv of 2,6-diphenylphenol, which features a lower steric profile, results in the quick formation of an intractable mixture of species, among which is Cp*IrH$_4$ (identified by ^{1}H NMR), most likely due to the competition in the protonolysis reactivities of the Al−C versus Al−Ir motifs together with ligand redistribution phenomena.

The Lewis acidity of the Al atom in complex **1** is confirmed by the coordination of pyridine, leading to the adduct [Cp*IrH$_3$Al(^{i}Bu)(OAr)(Py)] (**2**), which is isolated in 68% yield by cold crystallization in pentane (Scheme 5). The

Scheme 5. Reactivity of 1 with Pyridine

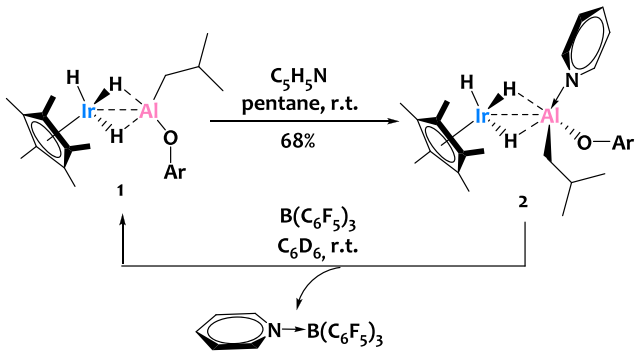

coordinated pyridine molecule can be dissociated from Al upon treatment of **2** with B(C$_6$F$_5$)$_3$, to restore complex **1** (Figure S11). The molecular structure of complex **2** is underpinned by multinuclei NMR and IR spectroscopy, elemental analysis, and X-ray diffraction analysis. The ^{1}H NMR spectrum of **2** is for the most part similar to that of **1** with a typically shielded hydride signal integrating for 3H at δ −17.26 ppm. Characteristic metal−hydride stretches around 2100 cm^{-1} are found in the DRIFT spectrum of **2**.

The solid-state molecular structure of **2** (Figure 2) confirms the N-coordination of the pyridine onto aluminum, with an Al1−N1 bond length (2.032(7) Å) in the expected range.[16,39] The Al cation adopts a pseudotetrahedral geometry with angles lying in the 92.6(3)−119.9(2)° range. The pyridine donation to Al results in an elongation of both the Al1−O1 bond (1.695(4) Å in **1** vs 1.776(6) Å in **2**) and the Al1···Ir1 distance from 2.406(2) Å in **1** to 2.502(2) Å in **2**. Note that the formal shortness ratio for the Ir−Al parameter (r = 0.998)[41] is at unity, indicating a strong interaction between the Cp*IrH$_3$ and Al(^{i}Bu)(OAr)(Py) fragments. The acute bending of the Cp* ring with respect to the Ir−Al axis (Cp*$_{centroid}$−Ir−Al angle of 138.73° in **2** vs 143.79° in **1**) suggests a terminal coordination of at least one of the hydrides.

Structural Investigation via DFT. In order to get better insights into the nature of the Ir−Al interaction in complexes **1** and **2** as well as to verify the position and role of the hydrides in the bonding, DFT calculations (B3PW91) were carried out. The bonding situations are very similar in **1** and **2** (see Figure

https://doi.org/10.1021/jacs.1c01725
J. Am. Chem. Soc. XXXX, XXX, XXX−XXX

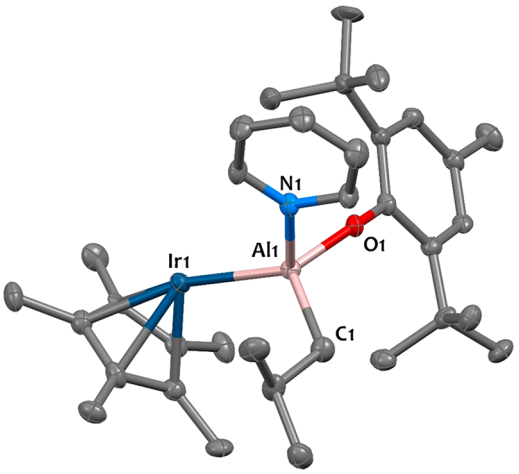

Figure 2. Solid-state molecular structure of **2**. Displacement ellipsoids are plotted at the 30% probability level. Hydrogen atoms have been omitted for clarity. Selected bond distances (Å) and angles (deg): Ir1−Al1 2.502(2), Al1−O1 1.776(6), Al1−C1 1.986(9), Al1−N1 2.032(7), O1−Al1−Ir1 119.9(2), O1−Al1−N1 92.6(3), O1−Al1−C1 113.2(3), N1−Al1−Ir1 113.2(2), C11−Al1−Ir1 114.4(3), C1−Al1−N1 99.4(3), Al1−Ir1−Cp*$_{centroid}$ 138.7(2).

S37 in the Supporting Information), and therefore hereafter only the description of **2** is given. Two isoenergetic structures are found for **2** (Figure 3), so that a rapid exchange of the

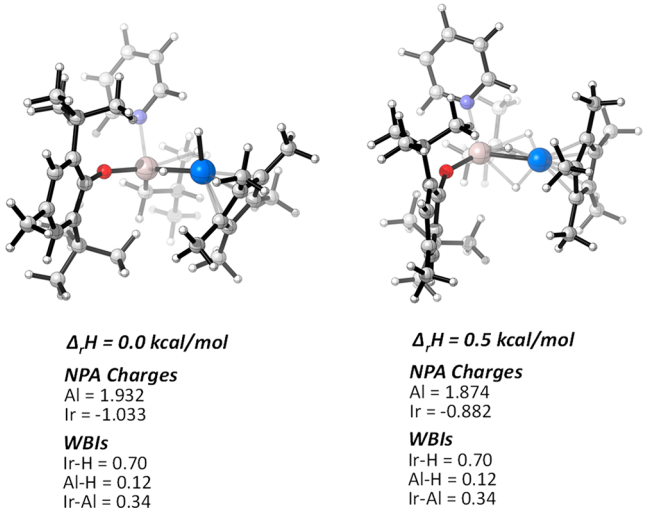

Figure 3. Calculated structures, NPA charges, and Wiberg bond indexes for the two conformers of complex **2**.

hydrides in solution is expected, which is in agreement with the ^{1}H NMR data. The most stable structure exhibits two bridging hydrides and one terminal Ir−H, whereas the three hydrogens have a μ-coordination in the second isomer (+0.5 kcal/mol). Interestingly, the presence of a terminal hydrogen has an effect on the geometry around the iridium center since the Al−Ir−X (X = Cp* centroid) angle is 136°, whereas this angle is 180° in the second isomer. The former geometry and the computed Ir−Al distance (2.51 Å computed vs 2.50 Å experimental) are in line with the X-ray crystallographic structure. Natural bonding orbital (NBO) analyses of the two isomers clearly indicate the presence of three covalent Ir−H interactions (with 50−58% contribution from the Ir spd hybrid orbital). At the second-order donor−acceptor level, donations from the Ir−H bonds as well from the Ir d lone pairs into the Al empty sp orbital are observed, in line with the presence of three-center−two-electron (3c-2e) Ir−H−Al bonds as well as some Ir−Al interactions. The latter is corroborated by an analysis of the Wiberg bond indexes (WBIs, Figure 3). The Ir−H WBIs are around 0.7, in line with a mainly covalent interaction, whereas the Al−H WBIs are close to 0.12−0.15, in line with electron delocalization from the Ir−H bond onto an acceptor orbital on Al. Interestingly, the Ir−Al WBI is around 0.3, in line with some bonding interaction between Ir and Al. The NPA charge on iridium is significant in both cases, taking values of −1.033 and −0.882, respectively, while the effective charges on the aluminum centers are +1.932 and +1.874, respectively (Figure 3). This analysis is consistent with the works of Crimmin and Aldridge on related M−Al (M = Rh, Au) complexes. Indeed, a substantial negative charge on the transition metal was reported in these cases, as well as similar WBIs.[15,19] These data support the description of **1** and **2** as containing a strongly polarized iridate(III) core, stabilized by Ir−H donation to the $[Al(^iBu)(OAr)Py_x]^+$ (x = 0, 1) fragment. This formalism is also consistent with the Pauling electronegativity gap between iridium and aluminum (2.20 vs 1.61, respectively). The strong polarity of these $Ir^{\delta-}$−$Al^{\delta+}$ pairs results in a substantial nucleophilic character of the Ir center, as confirmed by the reactivity studies described below.

Reactivity with Heteroallenes. Next, we probed the reactivity of these $Al^{\delta+}$−$Ir^{\delta-}$ derivatives toward electrophiles, and we first targeted carbon dioxide, given the importance of CO_2 activation by transition metals.[45,46] NMR monitoring of the reaction of **1** with CO_2 shows that a reaction occurs at room temperature, yet a complex mixture of species is formed. Among them, Cp*Ir(CO)H$_2$[47] and Cp*IrH$_4$[34] have been unambiguously identified. Unstable aluminum−oxo coproducts are most likely formed in the process and might explain why this reaction affords multiple products. Gratifyingly, the coordination of the pyridine Lewis base to Al does not quench the reactivity of the Ir−Al motif and helps stabilize the resulting Al derivatives, leading to cleaner reactions that are easier to decipher. Indeed, treatment of **2** with CO_2 (0.8 atm, 10 equiv, rt) leads to the clean reductive cleavage of CO_2, affording the iridium carbonyl species Cp*Ir(CO)H$_2$,[47] together with Cp*IrH$_4$[34] (see Figure S13) and the aluminum−oxo coproduct $[(i\text{Bu})(\text{OAr})\text{Al(Py)}]_2(\mu\text{-O})$ (**3**), which is isolated in 86% yield (Scheme 6).

The solid-state structure of **3** is shown in Figure 4. The two tetracoordinate Al atoms are connected by a bridging oxo group in a nearly linear fashion (Al1−O1−Al2 angle of 174.4(1)°). The substituents at the tetrahedral Al sites adopt

Scheme 6. Reactivity of 2 with CO_2

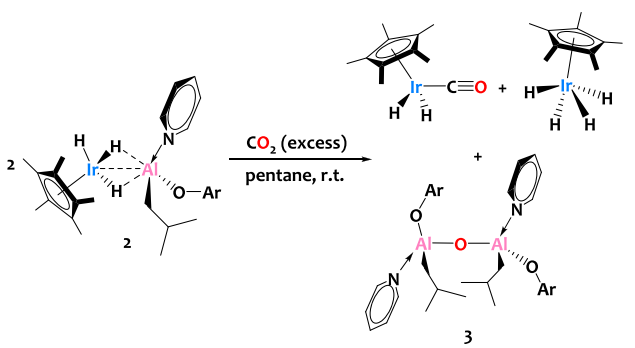

https://doi.org/10.1021/jacs.1c01725
J. Am. Chem. Soc. XXXX, XXX, XXX−XXX

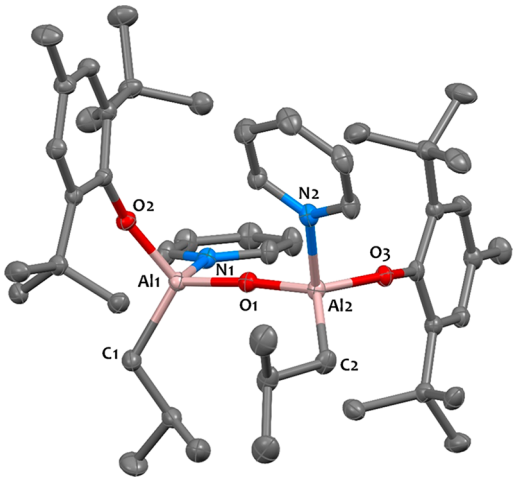

Figure 4. Solid-state molecular structure of **3**. Displacement ellipsoids are plotted at the 30% probability level. Hydrogen atoms have been omitted for clarity. Selected bond distances (Å) and angles (deg): Al1−O1 1.697(2), Al1−O2 1.744(2), Al1−C1 1.971(3), Al1−N1 2.006(2), Al2−O1 1.701(2), Al2−O3 1.750(2), Al2−C2 1.977(3), Al2−N2 2.005(2), Al1−O1−Al2 174.4(1).

an eclipsed conformation, with the two isobutyl ligands pointing in the same direction. The Al1−O1 and Al2−O1 bond distances (1.697(2) and 1.701(2) Å, respectively) are in the expected range.[48,49] A DRIFT spectroscopy analysis of **3** shows the absence of O−H vibrations, in agreement with a bridging oxo ligand (versus a bridging hydroxo). Note that, in solution, complex **3** exists as a mixture of two rotamers in a ratio of 93/7 which interconvert above 84 °C, as proved by a variable-temperature ^{1}H NMR experiment (see Figure S15).

Despite the pivotal role of methylaluminoxane derivatives in catalysis, very few well-defined alkylaluminoxanes are known to date. This can be attributed to the hydrolytic conditions classically used to prepare such derivatives, which are extremely difficult to control, together with the propensity of Al−O linkages to oligomerize to form insoluble amorphous materials. Complex **3** thus adds to the handful of structurally characterized molecular aluminum oxide species.[48−54] Note that examples of stoichiometric CO_2 reduction by low-valent Al species leading to C−O bond cleavage to yield CO + Al oxo/carbonate species have emerged only recently.[53−55] Here the reaction mechanism is totally different, since it does not involve redox changes of the Al(III) center (see DFT calculations below) but still allows the preparation of an unconventional Al−oxo species without having to isolate the low-valent Al derivative, which is remarkable. While insertion of CO_2 into polar metal−metal bonds[19,56−58] and main-group Lewis pairs[59−61] has been reported, to our knowledge the reductive cleavage of CO_2 leading to CO and O^{2-} by heterobimetallic systems has been described in only two occurrences. Thomas described the oxidative addition of CO_2 onto a Zr−Co bond, affording a (OC)Co(μ-O)Zr species, and Mazzanti described the CO_2 cleavage to CO gas and a U(V) oxo species involving a bimetallic uranium−potassium cooperative mechanism.[56,62]

This bimetallic reductive cleavage of CO_2 pushed us to explore further the reactivity of complex **2** toward other heteroallenes. Treatment of **2** with 2 equiv of adamantyl isocyanate results in the cleavage of the N=C bond to produce Cp*Ir(CO)H_2 and the aluminum ureate species {Al(OAr)(^{i}Bu)[κ^2-(N,O)AdNC(O)NHAd]} (**4**) (Scheme 7, top). Note that when only 1 equiv of AdNCO is used, an

Scheme 7. Reactivity of 2 with Heteroallenes

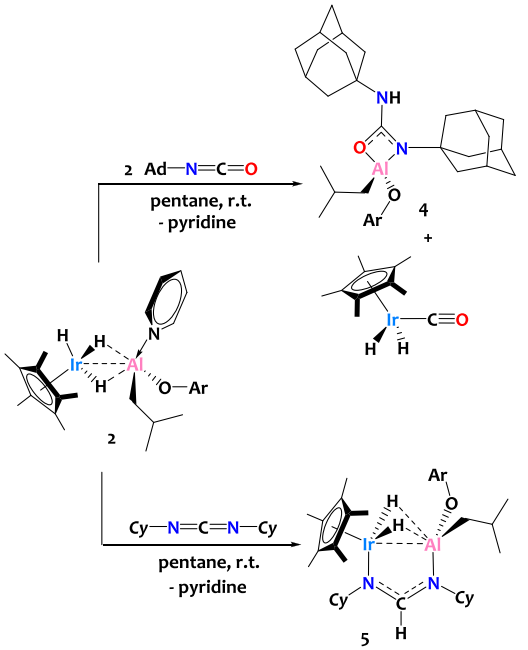

equimolar mixture of **2** and **4** is obtained (Figure S21). The ^{1}H NMR spectrum for **4** displays a distinctive singlet at δ +4.40 ppm attributed to the NH proton from the ureate ligand. The ^{13}C resonance corresponding to the ureate central carbon appears at a diagnostic chemical shift (δ +164.0 ppm) that is in agreement with literature data.[63] A typical ν(N−H) stretch is found at 3448 cm^{-1} in the DRIFT spectrum of **4**. The solid-state molecular structure of **4** as determined by X-ray diffraction is shown in Figure 5. The complex is four-coordinate, with a κ^2-ureate ligand arranged to favor the typical tetrahedral geometry around Al (O1−Al1−O2 = 109.36(8)°). The ureate ligand is bound to Al in a nonsymmetrical fashion, where the Al1−O1 bond length (1.863(2) Å) is shorter than the Al1−N1 length (1.911(2) Å), as in previously characterized ureate complexes.[63,64] The planarity of the [OCN_2] ureate core and the short O−C (1.309(4) Å) and N−C (1.331(3) and 1.341(3) Å) distances are consistent with electron delocalization and compare well with reported values for metal-bound ureates.[63,64]

By analogy with the reaction with CO_2 and in agreement with computational data (see below), we postulate that this aluminum ureate complex arises from a transient Al−amido species generated after CO extrusion. Complex **4** might thus arise from isocyanate insertion into such an Al−NHAd intermediate. Overall, this uncommon reaction adds to the handful of examples of the metal-mediated decarbonylation of isocyanates and cyanates.[65−69]

The reaction of **2** with dicyclohexylcarbodiimine does not lead to the reductive cleavage of a C=N bond but instead to the formation of a bridged amidinate species, Cp*IrH_2(μ-CyNC(H)NCy)Al(^{i}Bu)(OAr) (**5**) (Scheme 7, bottom), arising from hydride transfer to the central carbon of the heteroallene. The protonation of the central carbon of the amidinate is confirmed by NMR spectroscopy: the ^{1}H NMR spectrum for **5** displays a characteristic singlet at δ +6.99 ppm

https://doi.org/10.1021/jacs.1c01725
J. Am. Chem. Soc. XXXX, XXX, XXX−XXX

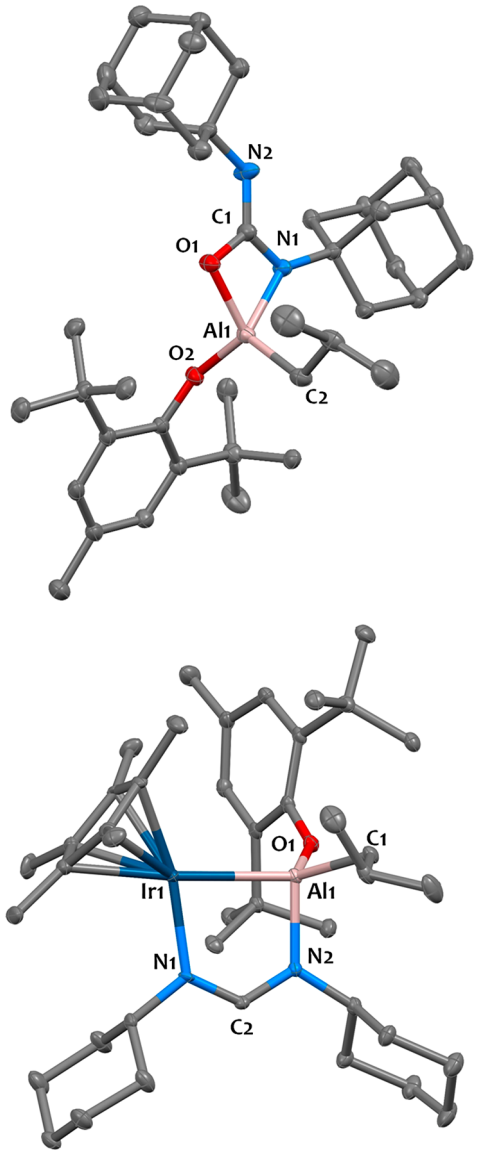

Figure 5. Solid-state molecular structures of **4** (top) and **5** (bottom). Displacement ellipsoids are plotted at the 30% probability level. Hydrogen atoms have been omitted for clarity. Selected bond distances (Å) and angles (deg): for **4**, Al1−O1 1.863(2), Al1−O2 1.710(2), Al1−C2 1.961(3), Al1−N1 1.911(2), N1−C1 1.331(3), N2−C1 1.341(3), O1−C1 1.309(4), N1−C1−O1 111.7(2), N1−C1−N2 127.8(2), O1−Al1−N1 70.73(7), O1−Al1−O2 109.36(8); for **5**, Ir1−Al1 2.617(1), Al1−O1 1.766(4), Al1−C1 1.986(5), Al1−N2 1.905(4), Ir1−N1 2.088(4), N1−C2 1.311(6), N2−C2 1.328(6), N1−C2−N2 124.8(4), N2−Al1−Ir1 91.0(1), O1−Al1−C1 107.5(2), N1−Ir1−Al1 81.2(1), Al1−Ir1−$Cp^*_{centroid}$ 144.85(1).

which correlates in the $^1H-^{13}C$ HSQC NMR experiment to the diagnostic ^{13}C resonance found at δ +162.9 ppm.

The crystallographic structure of **5** is shown in Figure 5. The bridging μ-η^1,η^1 amidinate ligand is located parallel to the metal−metal axis, as is commonly found in metal−metal-bonded dinuclear amidinate species.[70−72] This results in an elongation of the Ir···Al distance to 2.617(1) Å (versus 2.502(2) Å in **2**). The five-membered Ir1−Al1−N2−C2−N1 ring is almost perfectly planar, and the N1−C2 and N2−C2 bond distances (1.311(6) and 1.328(6) Å, respectively) are in the expected range for an amidinate motif.[72,73] The N1−C2−N2 angle (124.8(4)°) is much larger than that classically found in η^2 amidinates, but this value compares well with that reported for μ-η^1,η^1 amidinates bridging heavy-metal ions.[72,74] The N1−Ir1 (2.088(4) Å) and N2−Al1 (1.905(4) Å) bond lengths are comparable to those found in Al and Ir amidinate complexes, respectively.[20,75−77]

In order to better understand the reaction mechanisms operating in these heteroallene activations by Ir−Al metal−metal pairs, we carried out DFT calculations (B3PW91). The reaction begins by the replacement of the pyridine by a CO_2 molecule that binds to Al and Ir (Figure 6). This substitution is endothermic by 7.5 kcal/mol. From this adduct, the CO_2 undergoes a nucleophilic attack by the iridium center. Indeed, at the transition state (TS), the CO_2 molecule is bent in order to overlap an empty orbital at the carbon of CO_2 with a lone pair of the iridium center (see the associated molecular orbital in Figure S38 in the Supporting Information). The aluminum center ensures an electrophilic assistance by binding to the oxygen. The associated barrier is 18.9 kcal/mol, in line with a kinetically accessible reaction. From the intrinsic reaction coordinates, this yields a four-membered metallacyclic species whose formation is slightly endothermic (+3.6 kcal/mol) with respect to the reactants. Next, the small size of the CO_2 molecule allows a migratory insertion onto the Ir−Al bond. This is easily achieved through a low-lying TS (barrier of 10.5 kcal/mol) and leads to the formation of a stable metal-lacarboxylate complex (−11.5 kcal/mol) where the two oxygens bind to Al while C is bound to Ir. This intermediate is similar to the few examples where CO_2 is reductively inserted in polar metal−metal bonds.[19,58]

The presence of three hydrides on the Ir center, in close vicinity to the inserted CO_2, allows an easy hydrogen migration from Ir to one of the oxygen atoms. This migration occurs through a kinetically accessible TS (barrier of 25.8 kcal/mol), which is followed by a C−O bond breaking TS to ultimately yield the formation of an Al hydroxide molecule and $Cp^*Ir(CO)H_2$, whose formation is exothermic by 7.1 kcal/mol with respect to the reactants (the hydrogen transfer + CO bond breaking step being slightly endothermic by 4.4 kcal/mol from the $Ir(CO_2)Al$ carboxylate intermediate). The Al hydroxide species can then react with a second equivalent of complex **2**. This reaction is kinetically facile with a barrier of 13.4 kcal/mol and yields after pyridine recoordination the experimentally observed compounds **3** and Cp^*IrH_4. Other pathways were investigated (see Figure S39 in the Supporting Information) but the one reported here appears to be the most favorable. This CO_2 reduction mechanism is very different from that reported by Murray et al. for a diiron−hydride complex,[78] where the first step is a hydrogen transfer to CO_2, or the reaction reported by Lu et al.[79] using nickelate−group 13 complexes, where a CO_2 disproportionation is observed. On the other hand, the reactivity is slightly reminiscent of what is observed in f-element chemistry,[62,80−85] in particular with the formation of an intermediate where CO_2 is inserted between Ir and Al, but the protonation of CO_2 and the formation of a terminal hydroxyl unit are unique. Conceptually, the chemistry observed here is related to the heteroallene dipolar addition chemistry in Fisher carbene,[86−90] silylene,[91−95] or boryl[96] complexes, for instance in the case where CO_2 is added across a Ir=C(H)(OR) fragment, which is nucleophilic at Ir and electrophilic at C, leading to an iridium carbonyl adduct and HC(O)OR.[87]

Similar calculations were conducted for the reaction of **2** with AdNCO (Figure 7 and Figure S40). The reaction

https://doi.org/10.1021/jacs.1c01725
J. Am. Chem. Soc. XXXX, XXX, XXX−XXX

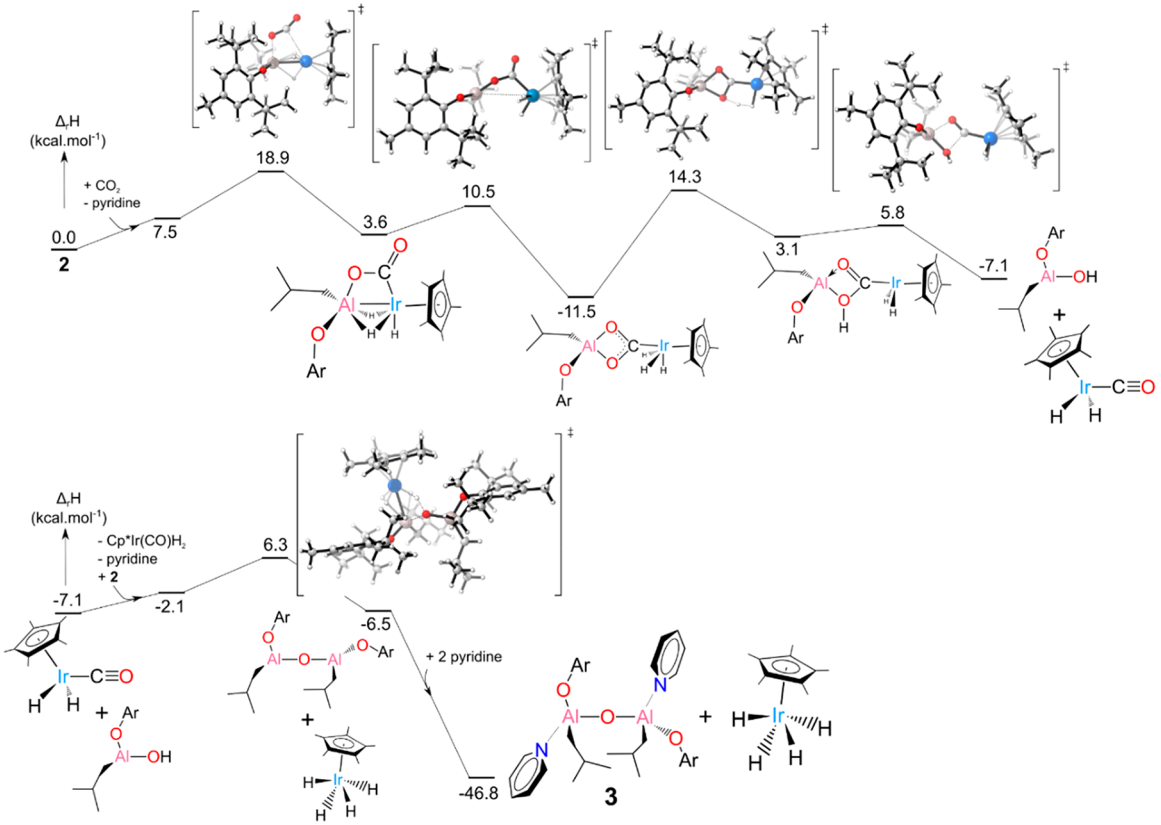

Figure 6. Computed enthalpy profile for the reaction of CO_2 with **2** at room temperature.

sequence is quite similar to that reported for CO_2. In particular, the replacement of pyridine by AdNCO is endothermic by 9.7 kcal/mol. From this adduct, AdNCO also undergoes a kinetically accessible (23.2 kcal/mol) nucleophilic attack by the Ir center, yielding an unstable four-membered metallacyclic intermediate (+7.2 kcal/mol). The next step is different from that reported for CO_2 and is likely due to the steric bulk of the adamantyl group. Indeed, AdNCO cannot easily insert between Ir and Al, so that the hydrogen transfer from Ir to N occurs on the four-membered-ring metallcycle with a barrier of 27.7 kcal/mol (hydride transfer to the oxygen and AdNCO insertion followed by hydrogen transfer were also computed and were found not to be competitive; see Figures S40 and S41). This hydrogen transfer is followed by a C−N bond breaking TS (barrier of 4.7 kcal/mol), which allows the formation of an Al amido complex and a molecule of $Cp^*Ir(CO)H_2$ (exothermic by 2.3 kcal/mol with respect to the reactants). The formed Al amide molecule does not react with a molecule of **2** (as observed with CO_2), presumably due to its steric bulk, but rather undergoes a [2 + 2] cycloaddition with another molecule of AdNCO (barrier of 6.9 kcal/mol). This yields a stable cycloaddition product (−23.1 kcal/mol), which can rearrange to a more stable isomer (−45.2 kcal/mol) through, for example, a 1,3-hydrogen shift. While isocyanates are well-known to undergo catalytic polymerization or cyclotrimerization,[97−101] selective dimerization of isocyanates to substituted ureas after the elimination of CO has been almost unexplored[102−104] and, to our knowledge, this original cooperative decarbonylation mechanism of AdNCO is unprecedented.

Calculations were also carried out on the reaction of **2** with CyN═C═NCy (see Figure S42). In that case the increased steric bulk stops the reaction at the amidinate complex, as observed experimentally.

CONCLUSION

In summary, the iridium tetrahydride complex Cp^*IrH_4 reacts with isobutylaluminum aryloxy derivatives to give unusual iridium aluminum species via a reductive elimination route. Spectroscopic, crystallographic, and computational data support the description of these heterobimetallic complexes as featuring strongly polarized $Al(III)^{\delta+}-Ir(III)^{\delta-}$ cores. Reactivity studies demonstrate that the Al sites retain their Lewis acidic character and that the binding of a Lewis base to Al does not quench the reactivity of the Ir−Al motif. More importantly, these Ir−Al species promote the cooperative reductive cleavage of heteroallenes (CO_2, AdNCO). In these processes, the Ir(III) center acts as a nucleophile. Although some Ir(I) species are known to act as nucleophiles,[88,105−109] to the best of our knowledge such behavior is unusual for d^6 Ir(III) complexes and thus such a result opens up attractive prospects for reactivity in catalysis. From the perspective of aluminum, these complexes allow access to unconventional motifs in molecular Al chemistry (e.g., oxos) without a change in the formal oxidation state of the Al(III) center. This contrasts with CO_2 cleavage promoted by low-oxidation-state aluminum species,[53−55] which are notoriously difficult to isolate, and thus represents a major achievement. This work also illustrates the multifaceted reactivity of transition metals toward alkylaluminum reagents, which are employed as cocatalysts in numerous processes. Future efforts will be devoted in our group to further explore the cooperative heterobimetallic reactivity of these unconventional molecular objects.

https://doi.org/10.1021/jacs.1c01725
J. Am. Chem. Soc. XXXX, XXX, XXX−XXX

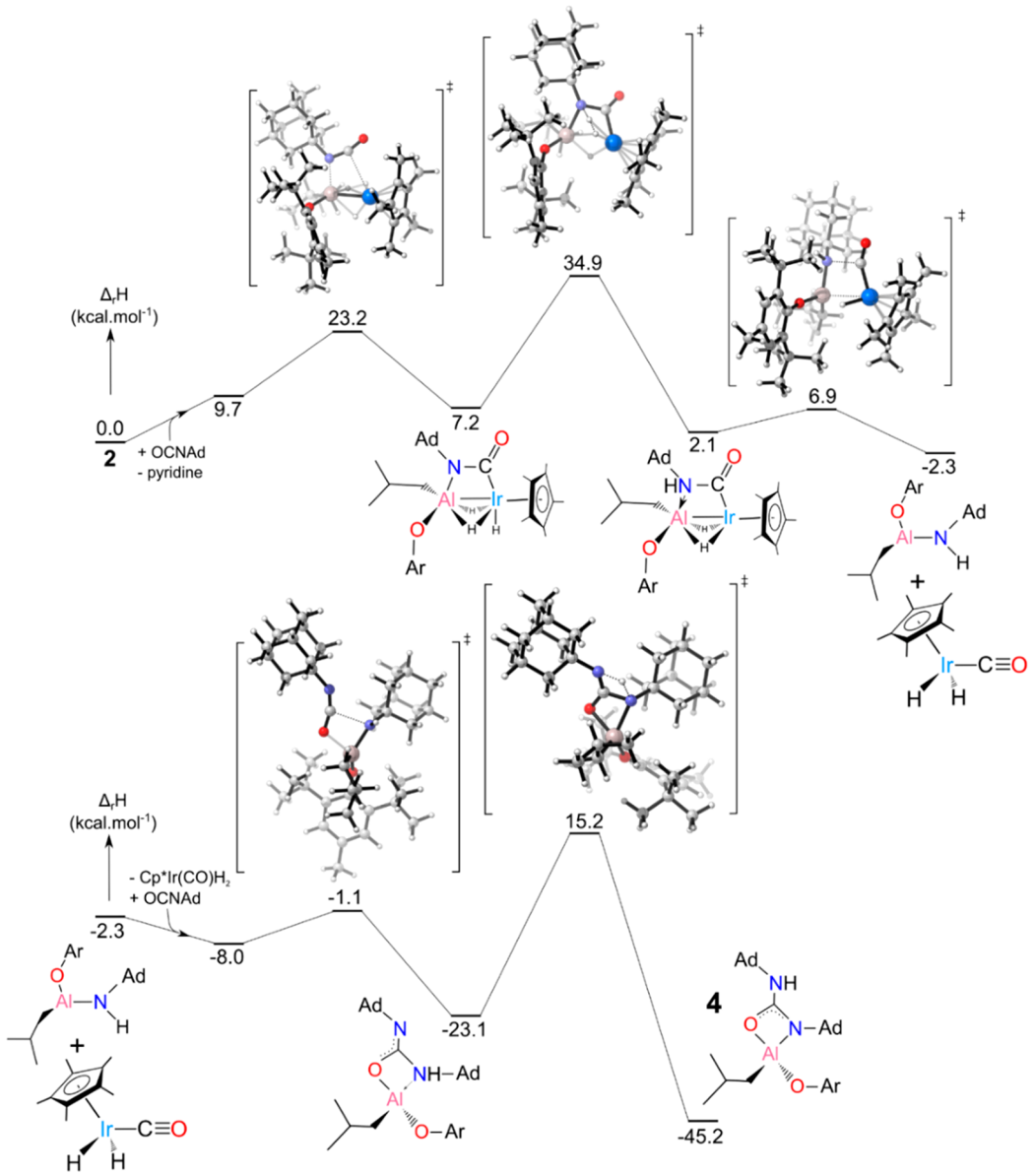

Figure 7. Computed enthalpy profile for the reaction of AdNCO with **2** at room temperature.

EXPERIMENTAL SECTION

General Considerations. Unless otherwise noted, all reactions were performed either using standard Schlenk line techniques or in an MBraun glovebox under an atmosphere of purified argon (<1 ppm of O_2/H_2O). Glassware and cannulas were stored in an oven at ~100 °C for at least 12 h prior to use. Toluene, *n*-pentane, octane, THF, and diethyl ether were purified by passage through a column of activated alumina, dried over Na/benzophenone, vacuum-transferred to a storage flask, and freeze−pump−thaw degassed prior to use. Deuterated solvents (THF-d_8, toluene-d_8, and C_6D_6) were dried over Na/benzophenone, vacuum-transferred to a storage flask, and freeze−pump−thaw degassed prior to use. CO_2 gas was dried over freshly regenerated R311G BASF catalyst/molecular sieves (4 Å) prior to use. The compounds Cp^*IrH_4,[34] $Al(^iBu)(OAr)_2$,[43] and $Al(^iBu)_2(OAr)$[43] (Ar = 2,6-(^{t}Bu)-3-MeC_6H_2) were prepared according to the literature procedures. All other reagents were acquired from commercial sources and used as received.

IR Spectroscopy. Samples were prepared in a glovebox (diluted in dry KBr), sealed under argon in a DRIFT cell equipped with KBr windows, and analyzed on a Nicolet 670 FT-IR spectrometer.

Elemental Analyses. Elemental analyses were performed under an inert atmosphere at Mikroanalytisches Labor Pascher, Germany.

X-ray Structural Determinations. Experimental details regarding single-crystal XRD measurements are provided in the Supporting Information. CCDC 2059453−2059457 contain supplementary crystallographic data for this paper. These data can be obtained free of charge from The Cambridge Crystallographic Data Centre via www.ccdc.cam.ac.uk/structures.

NMR Spectroscopy. Solution NMR spectra were recorded on Bruker AV-300, AVQ-400, and AV-500 spectrometers. ^{1}H and ^{13}C chemical shifts were measured relative to residual solvent peaks, which were assigned relative to an external TMS standard set at 0.00 ppm. ^{19}F chemical shifts are reported relative to $BF_3{\cdot}OEt_2$ set at 0.00 ppm. ^{1}H and ^{13}C NMR assignments were confirmed by ^{1}H−^{1}H COSY, ^{1}H−^{13}C HSQC, and HMBC experiments.

Synthesis of [$Cp^*IrH_3Al(^iBu)(OAr)$] (1). A 4 mL pentane solution of $IrCp^*H_4$ (282.5 mg, 0.85 mmol, 1.0 equiv) was added dropwise to a 8 mL colorless pentane solution of (2,6-di-*tert*-butyl-4-methylphenoxy)diisobutylaluminum, $Al(^iBu)_2(OAr)$ (310.0 mg, 0.86 mmol, 1.0 equiv). The resulting solution was stirred at room temperature for 20 h. Then, the volatiles were removed under vacuum, yielding a white solid (550 mg of crude solid). This powder

https://doi.org/10.1021/jacs.1c01725
J. Am. Chem. Soc. XXXX, XXX, XXX−XXX

was dissolved in the minimum amount of pentane (ca. 7 mL), and the solution was filtered and stored at −40 °C for 16 h, yielding compound **1** as white microcrystals (390.0 mg, 72% yield). ^{1}H NMR (500 MHz, C_6D_6, 293 K): δ 7.18 (s, 2H, CH_{Ar}), 2.32 (s, 3H, CH_3-Ar), 2.15 (m, 1H, CH_{iBu}), 1.96 (s, 15H, CH_{3Cp*}), 1.65 (s, 18H, $CH_{3\text{-}tBu}$), 1.08 (d, $^3J_{HH}$ = 6.4 Hz, 6H, $CH_{3\text{-}iBu}$), 0.31 (d, $^3J_{HH}$ = 7.1 Hz, 2H, $CH_{2\text{-}iBu}$), −16.80 (s, 3H, H−Ir). $^{13}C\{^1H\}$ NMR (125 MHz, C_6D_6, 293 K): δ 155.46 (C_{Ar}), 138.18 (C_{Ar}), 126.41 (C_{Ar}), 126.10 (CH_{Ar}), 94.64, (C_{Cp*}), 35.00 (), 32.88 ($CH_{2\text{-}iBu}$), 32.18 (), 28.04 ($CH_{3\text{-}iBu}$), 25.93 (CH_{iBu}), 21.59 ($ArCH_3$), 11.04 ($CH_{3\text{-}Cp*}$). DRIFTS (293 K, cm^{-1}) σ 2946 (s, ν_{C-H}), 2916 (s, ν_{C-H}), 2877 (s, ν_{C-H}), 2857 (s, ν_{C-H}), 2144 (s, ν_{Ir-H}), 1973 (s, ν_{Ir-H}), 1464 (s), 1425 (s), 1297 (s), 1286 (s), 1262 (s). Anal. Calcd for $C_{29}H_{50}AlIrO$: C, 54.95; H, 7.95. Found: C, 54.96; H, 8.00.

Synthesis of [Cp*IrH$_3$Al(^{i}Bu)(OAr)(Py)] (2). A 0.5 mL colorless pentane solution of pyridine (15.6 mg, 0.20 mmol, 1.0 equiv) was added dropwise to a 8.5 mL light yellow pentane solution of **1** (123.5 mg, 0.20 mmol, 1.0 equiv). The resulting pale yellow solution was stirred at room temperature for 30 min. Then, the volatiles were removed under vacuum, yielding a crude off-white oily material. This crude material was dissolved in the minimum amount of pentane (ca. 1.5 mL), and the solution was filtered and stored at −40 °C for 16 h, yielding **2** as colorless needle crystals (94 mg, 68% yield). Colorless block single crystals of **2** suitable for XRD studies were grown by slow recrystallization of **2** in an octane/toluene (7/1) mixture at −40 °C within 48 h. ^{1}H NMR (500 MHz, C_6D_6, 293 K): δ 8.89 (d, 2H, $CH_{ortho\text{-}Py}$), 7.24 (s, 2H, CH_{Ar}), 6.73 (t, 1H, $CH_{para\text{-}Py}$), 6.43 (t, 2H, $CH_{meta\text{-}Py}$), 2.37 (s, 3H, CH_3-Ar), 2.03 (s, 15H, CH_{3Cp*}), 1.86 (m, 1H, CH_{iBu}), 1.61 (s, 18H, $CH_{3\text{-}tBu}$), 1.06 (bs, 6H, $CH_{3\text{-}iBu}$), 0.74 (d, 2H, $CH_{2\text{-}iBu}$, $^3J_{HH}$ = 6.9 Hz), −17.26 (s, 3H, H−Ir). $^{13}C\{^1H\}$ NMR (125 MHz, C_6D_6, 293 K): δ 157.02 (C_{Ar}), 149.63 ($CH_{ortho\text{-}Py}$), 139.15 ($CH_{para\text{-}Py}$), 126.31 (CH_{Ar}), 124.61 (C_{Ar}), 124.04 ($CH_{meta\text{-}Py}$), 93.50 (C_{Cp*}), 35.30 (C_{tBu}), 32.61 ($CH_{3\text{-}tBu}$), 31.61 ($CH_{2\text{-}iBu}$), 28.35 ($CH_{3\text{-}iBu}$), 26.58 (CH_{iBu}), 21.42 ($CH_{3\text{-}Ar}$), 11.29 ($CH_{3\text{-}Cp*}$). DRIFTS (293 K, cm^{-1}): σ 2962 (s, ν_{C-H}), 2912 (s, ν_{C-H}), 2860 (s, ν_{C-H}), 2128 (s, ν_{Ir-H}), 2109 (s, ν_{Ir-H}), 1611 (m), 1449 (m), 1265 (s). Anal. Calcd for $C_{35}H_{59}AlIrNO$: C, 57.66; H, 8.16; N, 1.92. Found: C, 57.11; H, 7.78; N, 1.99.

Reaction of 2 with B(C_6F_5)$_3$, Yielding Complex 1 and (Py)B(C_6F_5)$_3$. A 0.4 mL colorless C_6D_6 solution of tris-(pentafluorophenyl)borane (8.2 mg, 16.0 μmol, 1.0 equiv) was added to a 0.2 mL C_6D_6 solution of complex **2** (11.7 mg, 16.0 μmol, 1.0 equiv). The resulting light yellow solution was sealed under argon in a J. Young NMR tube and was kept at room temperature for 24 h. An analysis of the resulting reaction mixture by ^{1}H NMR and ^{19}F NMR spectroscopy showed a quantitative formation of complex **1** together with the (Py)B(C_6F_5)$_3$ adduct. The NMR data for (Py)B(C_6F_5)$_3$ are in agreement with the previously reported data.[110] ^{1}H NMR (300 MHz, C_6D_6, 293 K): δ 7.94 (d, $^3J_{HH}$ = 5.6 Hz, 2H, $CH_{ortho\text{-}Py}$), 6.57 (m, 1H, $CH_{para\text{-}Py}$), 6.23 (t, $^3J_{HH}$ = 7.2 Hz, 2H, $CH_{meta\text{-}Py}$). ^{19}F NMR (282 MHz, C_6D_6, 293 K): δ −131.5 (d, $^3J_{FF}$ = 20 Hz, 6F, CF_{ortho}), −155.4 (t, $^3J_{FF}$ = 21 Hz, 3F, CF_{para}), −162.7 (m, 6F, CF_{meta}).

Reaction of 2 with CO$_2$, Yielding [(*i*Bu)(OAr)Al(Py)]$_2$(μ-O) (3). Complex **2** (174 mg, 0.24 mmol, 1.0 equiv) was dissolved in 20 mL of pentane. The resulting solution was charged in one compartment of a two-sided Schlenk reaction vessel featuring two isolated 74 cm^3 chambers. This double-Schlenk vessel was sealed under argon, the pentane solution was frozen in liquid nitrogen, and then the whole system was evacuated (10^{-4} mbar). The two compartments were isolated from each other using a J. Young high-vacuum PTFE valve. Afterward, dry CO_2 (800 mbar, 2.43 mmol, 10.2 equiv) was introduced in the first compartment. Then, the J. Young valve was opened for 15 min to let CO_2 diffuse at room temperature from the first compartment into the pentane solution of **2** located in the second compartment and the system was left in this configuration for 5 days without any stirring. This procedure triggered the nucleation of **2** as colorless block-shaped crystals in a yellow solution. The yellow filtrate was removed from the flask and analyzed by NMR spectroscopy, which showed the equimolar formation of Cp*IrH$_4$ and Cp*Ir(CO)-H$_2$. The colorless crystals were extracted with 6.0 mL of toluene. Then, the volatiles were removed under vacuum for 3 h, yielding the complex **3**·C_7H_8 as a white powder (92 mg, 86% yield). In solution, two rotamers of complex **3** are in equilibrium at 293 K in a 7:93 ratio. ^{1}H NMR (500 MHz, C_6D_6, 293 K): δ rotamer #1 8.76 (m, 4H, $CH_{ortho\text{-}Py}$), 7.24 (s, 4H, CH_{Ar}), 6.81 (m, 2H, $CH_{para\text{-}Py}$), 6.51 (m, 4H, $CH_{meta\text{-}Py}$), 2.40 (s, 6H, CH_3-Ar), 1.64 (m, 2H, CH_{iBu}), 1.51 (s, 36H, $CH_{3\text{-}tBu}$), 0.97 (d, 6H, $CH_{3\text{-}iBu}$), 0.82 (d, 6H, $CH_{3\text{-}iBu}$), 0.69 (d, $^3J_{HH}$ = 5.8 Hz, 1H, $CH_{2\text{-}iBu}$), 0.66 (d, $^3J_{HH}$ = 5.6 Hz, 1H, $CH_{2\text{-}iBu}$), 0.60 (d, 1H, $CH_{2\text{-}iBu}$), 0.58 (d, 1H, $CH_{2\text{-}iBu}$); δ rotamer #2 8.61 (m, 4H, $CH_{ortho\text{-}Py}$), 7.24 (s, 4H, CH_{Ar}), 6.77 (m, 2H, $CH_{para\text{-}Py}$), 6.36 (m, 4H, $CH_{meta\text{-}Py}$), 2.44 (s, 6H, CH_3-Ar), 1.88 (m, 2H, CH_{iBu}), 1.42 (s, 36H, $CH_{3\text{-}tBu}$), 1.34 (d, $^3J_{HH}$ = 6.4 Hz, 6H, $CH_{3\text{-}iBu}$), 0.99 (d, $^3J_{HH}$ = 6.4 Hz, 6H, $CH_{3\text{-}iBu}$), 0.89 (d, $^3J_{HH}$ = 6.6 Hz, 1H, $CH_{2\text{-}iBu}$), 0.86 (d, $^3J_{HH}$ = 6.4 Hz, 1H, $CH_{2\text{-}iBu}$), 0.61 (d, $^3J_{HH}$ = 6.7 Hz, 1H, $CH_{2\text{-}iBu}$), 0.59 (d, $^3J_{HH}$ = 6.6 Hz, 1H, $CH_{2\text{-}iBu}$). $^{13}C\{^1H\}$ NMR (125 MHz, C_6D_6, 293 K): δ rotamer #1 156.40 (C_{Ar}), 149.38 ($CH_{ortho\text{-}Py}$), 140.48 ($CH_{para\text{-}Py}$), 139.12 (C_{Ar}), 126.01 (CH_{Ar}), 124.57 (C_{Ar}), 124.46 ($CH_{meta\text{-}Py}$), 34.96 (C_{tBu}), 31.61 ($CH_{3\text{-}tBu}$), 29.61 ($CH_{3\text{-}iBu}$), 28.68 ($CH_{3\text{-}iBu}$), 26.26 (CH_{iBu}), 24.40 ($CH_{2\text{-}iBu}$), 21.48 ($CH_{3\text{-}Ar}$). DRIFTS (293 K, cm^{-1}): σ 3101 (m, ν_{C-H}), 3022 (m, ν_{C-H}), 2948 (s, ν_{C-H}), 2913 (s, ν_{C-H}), 2855 (s, ν_{C-H}), 1616 (m), 1451 (s), 1423 (s), 1271 (s). Anal. Calcd for $C_{48}H_{74}Al_2N_2O_3$·C_7H_8: C, 75.65; H, 9.47; N, 3.21. Found: C, 75.42; H, 9.24; N, 3.24.

Synthesis of Compound 4. A 3 mL colorless toluene solution of 1-adamantyl isocyanate (82.5 mg, 0.47 mmol, 2.0 equiv) was added dropwise to a 8 mL colorless pentane solution of **2** (167 mg, 0.23 mmol, 1.0 equiv). The reaction mixture was stirred at room temperature for 24 h, yielding a brownish solution. Volatiles were removed *in vacuo*, yielding a brownish solid containing an equimolar mixture of Cp*IrH$_2$(CO) and complex **4** (ca. 240 mg). This solid was dissolved in the minimum amount of pentane (ca. 8 mL), and the solution was filtered and stored at −40 °C for 3 weeks, yielding **4** as colorless block crystals suitable for XRD analysis (110 mg, 76% yield). ^{1}H NMR (500 MHz, C_6D_6, 293 K): δ 7.27 (s, 2H, CH_{Ar}), 4.40 (s, 1H, NH), 2.37 (s, 3H, CH_3-Ar), 2.19 (m, 1H, CH_{iBu}), 1.88−1.98 (m, 18H, CH_{Ad} and $CH_{2\text{-}Ad}$), 1.72 (s, 18H, $CH_{3\text{-}tBu}$), 1.45−1.55 (m, 12H, $CH_{2\text{-}Ad}$), 1.22 (dd, 6H, $CH_{3\text{-}iBu}$), 0.59 (m, 2H, $CH_{2\text{-}iBu}$). $^{13}C\{^1H\}$ NMR (125 MHz, C_6D_6, 293 K): δ 163.96 (C_{ureate}) 154.47 (C_{Ar}), 138.59 (C_{Ar}), 126.13 (CH_{Ar}), 126.08 (C_{Ar}), 53.11 (C_{Ad}), 50.27 (C_{Ad}), 43.54 ($CH_{2\text{-}Ad}$), 42.82 ($CH_{2\text{-}Ad}$), 36.62 ($CH_{2\text{-}Ad}$), 36.37 ($CH_{2\text{-}Ad}$), 35.28 (C_{tBu}), 31.71 ($CH_{3\text{-}tBu}$), 29.94 (CH_{Ad}), 29.89 (CH_{Ad}), 28.45 ($CH_{3\text{-}iBu}$), 28.02 ($CH_{3\text{-}iBu}$), 26.66 (CH_{iBu}), 21.81 ($CH_{2\text{-}iBu}$), 21.58 ($CH_{3\text{-}Ar}$). DRIFTS (293 K, cm^{-1}): σ 3448 (m, ν_{N-H}), 2944 (s, ν_{C-H}), 2911 (s, ν_{C-H}), 2847 (s, ν_{C-H}), 1575 (s), 1451 (s), 1490 (m), 1429 (m), 1278 (m). Anal. Calcd for $C_{40}H_{63}AlN_2O_2$: C, 76.15; H, 10.07; N, 4.44. Found: C, 76.02; H, 10.12; N, 4.39.

Synthesis of Compound 5. A 3 mL colorless pentane/toluene (1/1) solution of *N*,*N*′-dicyclohexylcarbodiimide (44.5 mg, 0.22 mmol, 1.1 equiv) was added dropwise to a 6.5 mL colorless pentane solution of **2** (144.5 mg, 0.20 mmol, 1.0 equiv). The resulting solution was stirred and heated at T = 50 °C for 3 h, triggering a color change from colorless to yellow. The crude reaction mixture was then cooled to room temperature and stirred for 24 h. Volatiles were then removed *in vacuo*, yielding a crude yellow powder (ca. 150 mg). This solid was dissolved in the minimum amount of pentane (ca. 6 mL), and the solution was filtered and stored at −40 °C, yielding **5** as light yellow block crystals suitable for XRD analysis (100 mg, 60% yield). ^{1}H NMR (500 MHz, C_6D_6, 293 K): δ 7.24 (s, 2H, CH_{Ar}), 6.99 (s, 1H, $CH_{Amidinate}$), 3.37 (m, 1H, CH_{Cy}), 2.83 (m, 1H, CH_{Cy}), 2.41 (s, 3H, CH_3-Ar), 2.35 (d, 1H, $CH_{2\text{-}Cy}$), 2.32 (m, 1H, CH_{iBu}), 2.23 (d, 1H, $CH_{2\text{-}Cy}$), 1.80 (m, 2H, $CH_{2\text{-}Cy}$), 1.73 (s, 18H, $CH_{3\text{-}tBu}$), 1.66 (m, 2H, $CH_{2\text{-}Cy}$), 1.61 (s, 15H, CH_{3Cp*}), 1.54 (m, 2H, $CH_{2\text{-}Cy}$), 1.45 (d, $^3J_{HH}$ = 6.7 Hz, 3H, $CH_{3\text{-}iBu}$), 1.41 (d, $^3J_{HH}$ = 6.6 Hz, 3H, $CH_{3\text{-}iBu}$), 0.95−1.39 (10H, m, $CH_{2\text{-}Cy}$), 0.93 (d, $^3J_{HH}$ = 6.6 Hz, 2H, $CH_{2\text{-}iBu}$), −14.52 (s, 1H, H−Ir),), −14.99 (s, 1H, H−Ir). $^{13}C\{^1H\}$ NMR (125 MHz, C_6D_6, 293 K): δ 161.86 ($CH_{Amidinate}$), 157.63 (C_{Ar}), 139.62 (C_{Ar}), 125.96 (CH_{Ar}), 124.03 (C_{Ar}), 92.05 (C_{Cp*}), 69.61 (CH_{Cy}), 57.33 (CH_{Cy}), 36.72 ($CH_{2\text{-}Cy}$), 35.95 ($CH_{2\text{-}Cy}$), 35.76 (C_{tBu}), 35.57

https://doi.org/10.1021/jacs.1c01725
J. Am. Chem. Soc. XXXX, XXX, XXX−XXX

($CH_{2\text{-}Cy}$), 35.24 ($CH_{2\text{-}Cy}$), 34.46 ($CH_{2\text{-}iBu}$), 32.63 ($CH_{3\text{-}tBu}$), 29.13 ($CH_{3\text{-}iBu}$), 28.18 ($CH_{2\text{-}Cy}$), 26.97 ($CH_{2\text{-}Cy}$), 26.75 ($CH_{2\text{-}Cy}$) 26.73 ($CH_{2\text{-}Cy}$), 26.36 (CH_{iBu}), 26.32 ($CH_{2\text{-}Cy}$), 26.16 ($CH_{2\text{-}Cy}$), 21.41 ($CH_{3\text{-}Ar}$), 10.48 ($CH_{3\text{-}Cp^*}$). DRIFTS (293 K, cm^{-1}) σ 2949 (s, ν_{C-H}), 2915 (s, ν_{C-H}), 2851 (s, ν_{C-H}), 2145 (w, ν_{Ir-H}), 2071 (w, ν_{Ir-H}), 1614 (s, $\nu_{C=N}$), 1447 (m), 1421 (s), 1264 (s). Anal. Calcd for $C_{43}H_{76}AlIrN_2O$: C, 60.32; H, 8.95; N, 3.27. Found: C, 60.13; H, 8.84; N, 3.28.

■ ASSOCIATED CONTENT

Supporting Information

The Supporting Information is available free of charge at https://pubs.acs.org/doi/10.1021/jacs.1c01725.

NMR, IR, XRD and computational data (PDF)

Cartesian coordinates for the calculated structures (XYZ)

Accession Codes

CCDC 2059453−2059457 contain the supplementary crystallographic data for this paper. These data can be obtained free of charge via www.ccdc.cam.ac.uk/data_request/cif, or by emailing data_request@ccdc.cam.ac.uk, or by contacting The Cambridge Crystallographic Data Centre, 12 Union Road, Cambridge CB2 1EZ, UK; fax: +44 1223 336033.

■ AUTHOR INFORMATION

Corresponding Author

Clément Camp − *Laboratory of Catalysis, Polymerization, Processes and Materials, CP2M UMR 5128, Université de Lyon, Institut de Chimie de Lyon, CNRS, Université Lyon 1, F-69616 Villeurbanne, France;* orcid.org/0000-0001-8528-0731; Email: clement.camp@univ-lyon1.fr

Authors

Léon Escomel − *Laboratory of Catalysis, Polymerization, Processes and Materials, CP2M UMR 5128, Université de Lyon, Institut de Chimie de Lyon, CNRS, Université Lyon 1, F-69616 Villeurbanne, France;* orcid.org/0000-0001-7744-1048

Iker Del Rosal − *Université de Toulouse, CNRS, INSA, UPS, UMR 5215, LPCNO, F-31077 Toulouse, France*

Laurent Maron − *Université de Toulouse, CNRS, INSA, UPS, UMR 5215, LPCNO, F-31077 Toulouse, France;* orcid.org/0000-0003-2653-8557

Erwann Jeanneau − *Université de Lyon, Centre de Diffractométrie Henri Longchambon, 69100 Villeurbanne, France*

Laurent Veyre − *Laboratory of Catalysis, Polymerization, Processes and Materials, CP2M UMR 5128, Université de Lyon, Institut de Chimie de Lyon, CNRS, Université Lyon 1, F-69616 Villeurbanne, France*

Chloé Thieuleux − *Laboratory of Catalysis, Polymerization, Processes and Materials, CP2M UMR 5128, Université de Lyon, Institut de Chimie de Lyon, CNRS, Université Lyon 1, F-69616 Villeurbanne, France;* orcid.org/0000-0002-5436-2467

Complete contact information is available at: https://pubs.acs.org/10.1021/jacs.1c01725

Author Contributions

All authors have given approval to the final version of the manuscript.

Funding

We gratefully acknowledge financial support from the CNRS-MOMENTUM program. CalMip is acknowledged for a generous grant of computing time (CALMIP-EOS grant 0833).

Notes

The authors declare no competing financial interest.

■ ACKNOWLEDGMENTS

We thank Anne Baudouin, Christine Lucas, and Nesrine Oueslati for their help with the NMR spectroscopic analyses. We thank the anonymous reviewers for their very insightful comments during the revision process of this manuscript.

■ REFERENCES

(1) Chen, E. Y. X.; Marks, T. J. Cocatalysts for Metal-Catalyzed Olefin Polymerization: Activators, Activation Processes, and Structure-Activity Relationships. *Chem. Rev.* **2000**, *100* (4), 1391−1434.

(2) Kaminsky, W. Discovery of Methylaluminoxane as Cocatalyst for Olefin Polymerization. *Macromolecules* **2012**, *45* (8), 3289−3297.

(3) Amgoune, A.; Bourissou, D. σ-Acceptor, Z-Type Ligands for Transition Metals. *Chem. Commun.* **2011**, *47* (3), 859−871.

(4) Schulz, S. Organoaluminum Complexes with Bonds to S-Block, p-Block, d-Block, and f-Block Metal Centers. In *Topics in Organometallic Chemistry*; Springer: Berlin, Heidelberg, 2012; pp 59−90. DOI: 10.1007/3418_2012_33.

(5) Lai, Q.; Cosio, M. N.; Ozerov, O. V. Ni Complexes of an Alane/Tris(Phosphine) Ligand Built around a Strongly Lewis Acidic Tris(N-Pyrrolyl)Aluminum. *Chem. Commun.* **2020**, *56* (94), 14845−14848.

(6) Bauer, J.; Bertermann, R.; Braunschweig, H.; Gruss, K.; Hupp, F.; Kramer, T. New Metal-Only Lewis Pairs: Elucidating the Electronic Influence of N -Heterocyclic Carbenes and Phosphines on the Dative Pt-Al Bond. *Inorg. Chem.* **2012**, *51* (10), 5617−5626.

(7) Devillard, M.; Nicolas, E.; Ehlers, A. W.; Backs, J.; Mallet-Ladeira, S.; Bouhadir, G.; Slootweg, J. C.; Uhl, W.; Bourissou, D. Dative Au→Al Interactions: Crystallographic Characterization and Computational Analysis. *Chem. - Eur. J.* **2015**, *21* (1), 74−79.

(8) Rudd, P. A.; Liu, S.; Gagliardi, L.; Young, V. G.; Lu, C. C. Metal-Alane Adducts with Zero-Valent Nickel, Cobalt, and Iron. *J. Am. Chem. Soc.* **2011**, *133* (51), 20724−20727.

(9) Bajo, S.; Alférez, M. G.; Alcaide, M. M.; López-Serrano, J.; Campos, J. Metal-Only Lewis Pairs of Rhodium with s, p and d-Block Metals. *Chem. - Eur. J.* **2020**, *26* (70), 16833−16845.

(10) Braunschweig, H.; Gruss, K.; Radacki, K. Interaction between D- and p-Block Metals: Synthesis and Structure of Platinum-Alane Adducts. *Angew. Chem., Int. Ed.* **2007**, *46* (41), 7782−7784.

(11) Devillard, M.; Declercq, R.; Nicolas, E.; Ehlers, A. W.; Backs, J.; Saffon-Merceron, N.; Bouhadir, G.; Slootweg, J. C.; Uhl, W.; Bourissou, D. A Significant but Constrained Geometry Pt→Al Interaction: Fixation of CO2 and CS2, Activation of H2 and PhCONH2. *J. Am. Chem. Soc.* **2016**, *138* (14), 4917−4926.

(12) Cowie, B. E.; Tsao, F. A.; Emslie, D. J. H. Synthesis and Platinum Complexes of an Alane-Appended 1,1′-Bis(Phosphino)-Ferrocene Ligand. *Angew. Chem., Int. Ed.* **2015**, *54* (7), 2165−2169.

(13) Golden, J. T.; Peterson, T. H.; Holland, P. L.; Bergman, R. G.; Andersen, R. A. Adduct Formation and Single and Double Deprotonation of Cp*(PMe3)Ir(H)2 with Main Group Metal Alkyls and Aryls: Synthesis and Structure of Three Novel Ir-Al and Ir-Mg Heterobimetallics. *J. Am. Chem. Soc.* **1998**, *120* (1), 223−224.

(14) Lai, Q.; Bhuvanesh, N.; Ozerov, O. V. Unexpected B/Al Transelementation within a Rh Pincer Complex. *J. Am. Chem. Soc.* **2020**, *142* (50), 20920−20923.

(15) Ekkert, O.; White, A. J. P.; Toms, H.; Crimmin, M. R. Addition of Aluminium, Zinc and Magnesium Hydrides to Rhodium(III). *Chem. Sci.* **2015**, *6* (10), 5617−5622.

(16) Morisako, S.; Watanabe, S.; Ikemoto, S.; Muratsugu, S.; Tada, M.; Yamashita, M. Synthesis of A Pincer-IrV Complex with A Base-

Free Alumanyl Ligand and Its Application toward the Dehydrogenation of Alkanes. *Angew. Chem., Int. Ed.* **2019**, *58* (42), 15031−15035.
(17) Takaya, J.; Iwasawa, N. Synthesis, Structure, and Catalysis of Palladium Complexes Bearing a Group 13 Metalloligand: Remarkable Effect of an Aluminum-Metalloligand in Hydrosilylation of CO2. *J. Am. Chem. Soc.* **2017**, *139* (17), 6074−6077.
(18) Hara, N.; Saito, T.; Semba, K.; Kuriakose, N.; Zheng, H.; Sakaki, S.; Nakao, Y. Rhodium Complexes Bearing PAlP Pincer Ligands. *J. Am. Chem. Soc.* **2018**, *140* (23), 7070−7073.
(19) Hicks, J.; Mansikkamäki, A.; Vasko, P.; Goicoechea, J. M.; Aldridge, S. A Nucleophilic Gold Complex. *Nat. Chem.* **2019**, *11* (3), 237−241.
(20) Riddlestone, I. M.; Urbano, J.; Phillips, N.; Kelly, M. J.; Vidovic, D.; Bates, J. I.; Taylor, R.; Aldridge, S. Salt Metathesis for the Synthesis of M-Al and M-H-Al Bonds. *Dalton Trans.* **2013**, *42* (1), 249−258.
(21) Anand, B. N.; Krossing, I.; Nöth, H. Synthesis and X-Ray Crystal Structure of (Tmp)2Al-Fe(Cp)(CO)2: An Alanyl-Containing Iron Complex with a Tricoordinated Aluminum Atom. *Inorg. Chem.* **1997**, *36* (9), 1979−1981.
(22) Agou, T.; Yanagisawa, T.; Sasamori, T.; Tokitoh, N. Synthesis and Structure of an Iron-Bromoalumanyl Complex with a Tri-Coordinated Aluminum Center. *Bull. Chem. Soc. Jpn.* **2016**, *89* (10), 1184−1186.
(23) Mears, K. L.; Stennett, C. R.; Taskinen, E. K.; Knapp, C. E.; Carmalt, C. J.; Tuononen, H. M.; Power, P. P. Molecular Complexes Featuring Unsupported Dispersion-Enhanced Aluminum-Copper and Gallium-Copper Bonds. *J. Am. Chem. Soc.* **2020**, *142* (47), 19874−19878.
(24) Minasian, S. G.; Krinsky, J. L.; Williams, V. A.; Arnold, J. A Heterobimetallic Complex with an Unsupported Uranium(III)-Aluminum(I) Bond: (CpSiMe3)3U-AlCp* (Cp* = C 5Me5). *J. Am. Chem. Soc.* **2008**, *130* (31), 10086−10087.
(25) Altman, A. B.; Brown, A. C.; Rao, G.; Lohrey, T. D.; Britt, R. D.; Maron, L.; Minasian, S. G.; Shuh, D. K.; Arnold, J. Chemical Structure and Bonding in a Thorium(Iii)-Aluminum Heterobimetallic Complex. *Chem. Sci.* **2018**, *9* (18), 4317−4324.
(26) Koshino, K.; Kinjo, R. Construction of σ-Aromatic AlB 2 Ring via Borane Coupling with a Dicoordinate Cyclic (Alkyl)(Amino)-Aluminyl Anion. *J. Am. Chem. Soc.* **2020**, *142* (19), 9057−9062.
(27) Kurumada, S.; Takamori, S.; Yamashita, M. An Alkyl-Substituted Aluminium Anion with Strong Basicity and Nucleophilicity. *Nat. Chem.* **2020**, *12* (1), 36−39.
(28) Hicks, J.; Vasko, P.; Goicoechea, J. M.; Aldridge, S. The Aluminyl Anion: A New Generation of Aluminium Nucleophile. *Angew. Chem., Int. Ed.* **2021**, *60* (4), 1702−1713.
(29) Queen, J. D.; Lehmann, A.; Fettinger, J. C.; Tuononen, H. M.; Power, P. P. The Monomeric Alanediyl: AlAriPr8(AriPr8= C6H-2,6-(C6H2−2,4,6-Pr I3)2−3,5-Pr I2): An Organoaluminum(I) Compound with a One-Coordinate Aluminum Atom. *J. Am. Chem. Soc.* **2020**, *142* (49), 20554−20559.
(30) Golden, J. T.; Peterson, T. H.; Holland, P. L.; Bergman, R. G.; Andersen, R. A. Adduct Formation and Single and Double Deprotonation of Cp*(PMe3)Ir(H)2 with Main Group Metal Alkyls and Aryls: Synthesis and Structure of Three Novel Ir-Al and Ir-Mg Heterobimetallics. *J. Am. Chem. Soc.* **1998**, *120* (1), 223−224.
(31) Lassalle, S.; Jabbour, R.; Schiltz, P.; Berruyer, P.; Todorova, T. K.; Veyre, L.; Gajan, D.; Lesage, A.; Thieuleux, C.; Camp, C. Metal−Metal Synergy in Well-Defined Surface Tantalum−Iridium Heterobimetallic Catalysts for H/D Exchange Reactions. *J. Am. Chem. Soc.* **2019**, *141* (49), 19321−19335.
(32) Del Rosal, I.; Lassalle, S.; Dinoi, C.; Thieuleux, C.; Maron, L.; Camp, C. Mechanistic Investigations via DFT Support the Cooperative Heterobimetallic C-H and O-H Bond Activation across TaIr Multiple Bonds. *Dalton Trans.* **2021**, *50* (2), 504−510.
(33) Lassalle, S.; Jabbour, R.; Del Rosal, I.; Maron, L.; Fonda, E.; Veyre, L.; Gajan, D.; Lesage, A.; Thieuleux, C.; Camp, C. Stepwise Construction of Silica-Supported Tantalum/Iridium Heteropolymetallic Catalysts Using Surface Organometallic Chemistry. *J. Catal.* **2020**, *392*, 287−301.
(34) Gilbert, T. M.; Hollander, F. J.; Bergman, R. G. (Pentamethylcyclopentadienyl)Iridium Polyhydride Complexes: Synthesis of Intermediates in the Mechanism of Formation of (C5(CH3)5)IrH4 and the Preparation of Several Iridium(V) Compounds. *J. Am. Chem. Soc.* **1985**, *107* (12), 3508−3516.
(35) Findlater, M.; Schultz, K. M.; Bernskoetter, W. H.; Cartwright-Sykes, A.; Heinekey, D. M.; Brookhart, M. Dihydrogen Complexes of Iridium and Rhodium. *Inorg. Chem.* **2012**, *51* (8), 4672−4678.
(36) Rozenel, S. S.; Padilla, R.; Camp, C.; Arnold, J. Unusual Activation of H2 by Reduced Cobalt Complexes Supported by a PNP Pincer Ligand. *Chem. Commun.* **2014**, *50* (20), 2612−2614.
(37) Oishi, M.; Oshima, M.; Suzuki, H. A Study on Zr-Ir Multiple Bonding Active for C-H Bond Cleavage. *Inorg. Chem.* **2014**, *53* (13), 6634−6654.
(38) Morisako, S.; Watanabe, S.; Ikemoto, S.; Muratsugu, S.; Tada, M.; Yamashita, M. Synthesis of A Pincer-IrV Complex with A Base-Free Alumanyl Ligand and Its Application toward the Dehydrogenation of Alkanes. *Angew. Chem., Int. Ed.* **2019**, *58* (42), 15031−15035.
(39) Nakamura, T.; Suzuki, K.; Yamashita, M. Aluminabenzene-Rh and -Ir Complexes: Synthesis, Structure, and Application toward Catalytic C-H Borylation. *J. Am. Chem. Soc.* **2017**, *139* (49), 17763−17766.
(40) Pauling, L. Atomic Radii and Interatomic Distances in Metals. *J. Am. Chem. Soc.* **1947**, *69* (3), 542−553.
(41) Cotton, F. A.; Murillo, C. A.; Walton, R. A. *Multiple Bonds between Metal Atoms*, 3rd ed.; Cotton, F. A., Murillo, C. A., Walton, R. A., Eds.; Springer Science and Business Media: New York, 2005.
(42) Dardun, V.; Escomel, L.; Jeanneau, E.; Camp, C. On the Alcoholysis of Alkyl-Aluminum(III) Alkoxy-NHC Derivatives: Reactivity of the Al-Carbene Lewis Pair versus Al-Alkyl. *Dalton Trans.* **2018**, *47* (31), 10429−10433.
(43) Shreve, A. P.; Mulhauot, R.; Fultz, W.; Calabrese, J.; Robbins, W.; Ittel, S. D. Sterically Hindered Aryloxide-Substituted Alkylaluminum Compounds. *Organometallics* **1988**, *7* (2), 409−416.
(44) Nöth, H.; Schlegel, A.; Knizek, J.; Krossing, I.; Ponikwar, W.; Seifert, T. Lithium and Sodium Alkoxy- and Aryloxyhydridoaluminates in Solution and in the Solid State. *Chem. - Eur. J.* **1998**, *4* (11), 2191−2203.
(45) Appel, A. M.; Bercaw, J. E.; Bocarsly, A. B.; Dobbek, H.; Dubois, D. L.; Dupuis, M.; Ferry, J. G.; Fujita, E.; Hille, R.; Kenis, P. J. A.; et al. Frontiers, Opportunities, and Challenges in Biochemical and Chemical Catalysis of CO2 Fixation. *Chem. Rev.* **2013**, *113* (8), 6621−6658.
(46) Gibson, D. H. The Organometallic Chemistry of Carbon Dioxide. *Chem. Rev.* **1996**, *96* (6), 2063−2095.
(47) Heinekey, D. M.; Fine, D. A.; Harper, T. G. P.; Michel, S. T. Dinuclear Dihydride Complexes of Iridium: A Study of Structure and Dynamics. *Can. J. Chem.* **1995**, *73* (7), 1116−1125.
(48) Mason, M. R.; Barron, A. R.; Smith, J. M.; Bott, S. G. Hydrolysis of Tri-Tert-Butylaluminum: The First Structural Characterization of Alkylalumoxanes [(R2Al)2O]n and (RAlO)N. *J. Am. Chem. Soc.* **1993**, *115* (12), 4971−4984.
(49) Bai, G.; Roesky, H. W.; Li, J.; Noltemeyer, M.; Schmidt, H. G. Synthesis, Structural Characterization, and Reaction of the First Terminal Hydroxide-Containing Alumoxane with an [{Al(OH)]2(μ-O)] Core. *Angew. Chem., Int. Ed.* **2003**, *42* (44), 5502−5506.
(50) Neculai, D.; Roesky, H. W.; Neculai, A. M.; Magull, J.; Walfort, B.; Stalke, D. Formation and Characterization of the First Monoalumoxane, LAlO·B(C6F5)3. *Angew. Chem., Int. Ed.* **2002**, *41* (22), 4294−4296.
(51) Wehmschulte, R. J.; Power, P. P. A New Synthetic Route to Organoalumoxanes (RAlO)(n): Synthesis of (Mes* = AlO)4 (Mes* = -C6H2−2,4,6-t-Bu3) and Its Reactions with AIR3 (R = Me or Et). *J. Am. Chem. Soc.* **1997**, *119* (35), 8387−8388.
(52) Harlan, C. J.; Mason, M. R.; Barron, A. R. Tert-Butylaluminum Hydroxides and Oxides: Structural Relationship between Alkylalu-

https://doi.org/10.1021/jacs.1c01725
J. Am. Chem. Soc. XXXX, XXX, XXX−XXX

moxanes and Alumina Gels. *Organometallics* **1994**, *13* (8), 2957−2969.
(53) Hicks, J.; Heilmann, A.; Vasko, P.; Goicoechea, J. M.; Aldridge, S. Trapping and Reactivity of a Molecular Aluminium Oxide Ion. *Angew. Chem., Int. Ed.* **2019**, *58* (48), 17265−17268.
(54) Weetman, C.; Bag, P.; Szilvási, T.; Jandl, C.; Inoue, S. CO2 Fixation and Catalytic Reduction by a Neutral Aluminum Double Bond. *Angew. Chem., Int. Ed.* **2019**, *58* (32), 10961−10965.
(55) Anker, M. D.; Coles, M. P. Aluminium-Mediated Carbon Dioxide Reduction by an Isolated Monoalumoxane Anion. *Angew. Chem., Int. Ed.* **2019**, *58* (50), 18261−18265.
(56) Krogman, J. P.; Foxman, B. M.; Thomas, C. M. Activation of CO2 by a Heterobimetallic Zr/Co Complex. *J. Am. Chem. Soc.* **2011**, *133* (37), 14582−14585.
(57) Memmler, H.; Kauper, U.; Gade, L. H.; Scowen, I. J.; McPartlin, M. Insertion of X = C=Y Heteroallenes into Unsupported Zr-M Bonds (M = Fe, Ru). *Chem. Commun.* **1996**, No. 15, 1751−1752.
(58) Pinkes, J. R.; Steffey, B. D.; Vites, J. C.; Cutler, A. R. Carbon Dioxide Insertion into the Fe-Zr and Ru-Zr Bonds of the Heterobimetallic Complexes Cp(CO)2M-Zr(Cl)Cp2: Direct Production of the μ-H1(C):H2(O,O′)-CO2 Compounds Cp(CO)2M-CO2-Zr(Cl)Cp2. *Organometallics* **1994**, *13* (1), 21−23.
(59) Mömming, C. M.; Otten, E.; Kehr, G.; Fröhlich, R.; Grimme, S.; Stephan, D. W.; Erker, G. Reversible Metal-Free Carbon Dioxide Binding by Frustrated Lewis Pairs. *Angew. Chem., Int. Ed.* **2009**, *48* (36), 6643−6646.
(60) Ménard, G.; Stephan, D. W. Stoichiometric Reduction of CO2 to CO by Aluminum-Based Frustrated Lewis Pairs. *Angew. Chem., Int. Ed.* **2011**, *50* (36), 8396−8399.
(61) Ménard, G.; Stephan, D. W. Room Temperature Reduction of CO2 to Methanol by Al-Based Frustrated Lewis Pairs and Ammonia Borane. *J. Am. Chem. Soc.* **2010**, *132* (6), 1796−1797.
(62) Cooper, O.; Camp, C.; Pécaut, J.; Kefalidis, C. E.; Maron, L.; Gambarelli, S.; Mazzanti, M. Multimetallic Cooperativity in Uranium-Mediated CO2 Activation. *J. Am. Chem. Soc.* **2014**, *136* (18), 6716−6723.
(63) Leitch, D. C.; Schafer, L. L. Zirconium Alkyl Complexes Supported by Ureate Ligands: Synthesis, Characterization, and Precursors to Metal-Element Multiple Bonds. *Organometallics* **2010**, *29* (21), 5162−5172.
(64) Leitch, D. C.; Platel, R. H.; Schafer, L. L. Mechanistic Elucidation of Intramolecular Aminoalkene Hydroamination Catalyzed by a Tethered Bis(Ureate) Complex: Evidence for Proton-Assisted C-N Bond Formation at Zirconium. *J. Am. Chem. Soc.* **2011**, *133* (39), 15453−15463.
(65) Bock, H.; Breuer, O. Decarbonylation on Carbon-Supported Nickel Catalysts. *Angew. Chem., Int. Ed. Engl.* **1987**, *26* (5), 461−462.
(66) Joost, M.; Transue, W. J.; Cummins, C. C. Terminal Tungsten Pnictide Complex Formation through Pnictaethynolate Decarbonylation. *Chem. Commun.* **2017**, *53* (77), 10731−10733.
(67) Eller, K.; Schwarz, H. Reaction of Isopropyl Isocyanate with Bare Vanadium(I) Cations Leading to Combined Decarbonylation/Demethanation. *Inorg. Chem.* **1990**, *29* (17), 3250−3252.
(68) Fickes, M. G.; Odom, A. L.; Cummins, C. C. A Nucleophilic Niobium(V) Nitride Prepared by Isocyanate Decarbonylation. *Chem. Commun.* **1997**, No. 20, 1993−1994.
(69) Bonfada, É.; Abram, U.; Strähle, J. Synthese, Struktur Und Photolyse von Isocyanatokomplexen Des Rheniums. *Z. Anorg. Allg. Chem.* **1998**, *624* (5), 757−762.
(70) Sadique, A. R.; Heeg, M. J.; Winter, C. H. A Weak, Short Metal-Metal Bond in a Chromium(II) Amidinate Complex. *J. Am. Chem. Soc.* **2003**, *125* (26), 7774−7775.
(71) Cotton, F. A.; Daniels, L. M.; Murillo, C. A. The First Complex with a $\Sigma 2\pi 4$ Triple Bond between Vanadium Atoms in a Ligand Framework of Fourfold Symmetry—[V2{(P-CH3C6H4)NC(H)N-(P-C6H4CH3)}4]. *Angew. Chem., Int. Ed. Engl.* **1992**, *31* (6), 737−738.
(72) Leopold, H.; Tenne, M.; Tronnier, A.; Metz, S.; Münster, I.; Wagenblast, G.; Strassner, T. Binuclear ĈC* Cyclometalated Platinum(II) NHC Complexes with Bridging Amidinate Ligands. *Angew. Chem., Int. Ed.* **2016**, *55* (51), 15779−15782.
(73) Camp, C.; Settineri, N.; Lefèvre, J.; Jupp, A. R.; Goicoechea, J. M.; Maron, L.; Arnold, J. Uranium and Thorium Complexes of the Phosphaethynolate Ion. *Chem. Sci.* **2015**, *6* (11), 6379−6384.
(74) Zhou, Y.; Richeson, D. S. Synthesis and Structure of Novel Bridged Dinuclear Indium Complexes. *Inorg. Chem.* **1996**, *35* (6), 1423−1424.
(75) Dagorne, S.; Guzei, I. A.; Coles, M. P.; Jordan, R. F. Synthesis and Structures of Cationic Aluminum and Gallium Amidinate Complexes. *J. Am. Chem. Soc.* **2000**, *122* (2), 274−289.
(76) Brazeau, A. L.; Wang, Z.; Rowley, C. N.; Barry, S. T. Synthesis and Thermolysis of Aluminum Amidinates: A Ligand-Exchange Route for New Mixed-Ligand Systems. *Inorg. Chem.* **2006**, *45* (5), 2276−2281.
(77) Simpson, R. D.; Marshall, W. J. Syntheses and Structures of (Pentamethylcyclopentadienyl)Iridium Amidinate Complexes. *Organometallics* **1997**, *16* (16), 3719−3722.
(78) Hong, D. H.; Murray, L. J. Carbon Dioxide Insertion into Bridging Iron Hydrides: Kinetic and Mechanistic Studies. *Eur. J. Inorg. Chem.* **2019**, *2019* (15), 2146−2153.
(79) Vollmer, M. V.; Cammarota, R. C.; Lu, C. C. Reductive Disproportionation of CO_2 Mediated by Bimetallic Nickelate(-I)/Group 13 Complexes. *Eur. J. Inorg. Chem.* **2019**, *2019* (15), 2140−2145.
(80) Mougel, V.; Camp, C.; Pécaut, J.; Copéret, C.; Maron, L.; Kefalidis, C. E.; Mazzanti, M. Siloxides as Supporting Ligands in Uranium(III)-Mediated Small-Molecule Activation. *Angew. Chem., Int. Ed.* **2012**, *51* (49), 12280−12284.
(81) Schmidt, A.; Heinemann, F. W.; Kefalidis, C. E.; Maron, L.; Roesky, P. W.; Meyer, K. Activation of SO_2 and CO_2 by Trivalent Uranium Leading to Sulfite/Dithionite and Carbonate/Oxalate Complexes. *Chem. - Eur. J.* **2014**, *20* (42), 13501−13506.
(82) Formanuik, A.; Ortu, F.; Inman, C. J.; Kerridge, A.; Castro, L.; Maron, L.; Mills, D. P. Concomitant Carboxylate and Oxalate Formation From the Activation of CO_2 by a Thorium(III) Complex. *Chem. - Eur. J.* **2016**, *22* (50), 17976−17979.
(83) Castro, L.; Lam, O. P.; Bart, S. C.; Meyer, K.; Maron, L. Carbonate Formation from CO2 via Oxo versus Oxalate Pathway: Theoretical Investigations into the Mechanism of Uranium-Mediated Carbonate Formation. *Organometallics* **2010**, *29* (21), 5504−5510.
(84) Tsoureas, N.; Castro, L.; Kilpatrick, A. F. R.; Cloke, F. G. N.; Maron, L. Controlling Selectivity in the Reductive Activation of CO2 by Mixed Sandwich Uranium(Iii) Complexes. *Chem. Sci.* **2014**, *5* (10), 3777−3788.
(85) Camp, C.; Chatelain, L.; Kefalidis, C. E.; Pécaut, J.; Maron, L.; Mazzanti, M. CO2 Conversion to Isocyanate via Multiple N-Si Bond Cleavage at a Bulky Uranium(III) Complex. *Chem. Commun.* **2015**, *51* (84), 15454−15457.
(86) Whited, M. T.; Grubbs, R. H. A Catalytic Cycle for Oxidation of Tert-Butyl Methyl Ether by a Double C-H Activation-Group Transfer Process. *J. Am. Chem. Soc.* **2008**, *130* (49), 16476−16477.
(87) Whited, M. T.; Grubbs, R. H. Oxygen-Atom Transfer from Carbon Dioxide to a Fischer Carbene at (PNP)Ir. *J. Am. Chem. Soc.* **2008**, *130* (18), 5874−5875.
(88) Whited, M. T.; Grubbs, R. H. Late Metal Carbene Complexes Generated by Multiple C-H Activations: Examining the Continuum of M═C Bond Reactivity. *Acc. Chem. Res.* **2009**, *42* (10), 1607−1616.
(89) van der Boom, M. E. Oxygen Atom "Cut and Paste" from Carbon Dioxide to a Fischer Carbene Complex. *Angew. Chem., Int. Ed.* **2009**, *48* (1), 28−30.
(90) Brookes, N. J.; Ariafard, A.; Stranger, R.; Yates, B. F. Cleavage of Carbon Dioxide by an Iridium-Supported Fischer Carbene. A DFT Investigation. *J. Am. Chem. Soc.* **2009**, *131* (16), 5800−5808.
(91) Whited, M. T.; Zhang, J.; Conley, A. M.; Ma, S.; Janzen, D. E.; Kohen, D. Bimetallic, Silylene-Mediated Multielectron Reductions of

https://doi.org/10.1021/jacs.1c01725
J. Am. Chem. Soc. XXXX, XXX, XXX−XXX

Carbon Dioxide and Ethylene. *Angew. Chem., Int. Ed.* **2021**, *60* (3), 1615−1619.
(92) Price, J. S.; Emslie, D. J. H. Reactions of Manganese Silyl and Silylene Complexes with CO2and C(NiPr)2: Synthesis of Mn(I) Formate and Amidinylsilyl Complexes. *Organometallics* **2020**, *39* (24), 4618−4628.
(93) Whited, M. T.; Zhang, J.; Ma, S.; Nguyen, B. D.; Janzen, D. E. Silylene-Assisted Hydride Transfer to CO2 and CS2 at a [P2Si]Ru Pincer-Type Complex. *Dalton Trans.* **2017**, *46* (43), 14757−14761.
(94) Xie, H.; Lin, Z. Understanding the Reactivity Difference of Isocyanate and Isothiocyanate toward a Ruthenium Silylene Hydride Complex. *Organometallics* **2014**, *33* (4), 892−897.
(95) Ochiai, M.; Hashimoto, H.; Tobita, H. Reactions of a Neutral Silylene Ruthenium Complex with Heterocumulenes: C = o Hydrosilylation of Isocyanates vs C = s Bond Cleavage of Isothiocyanate. *Organometallics* **2012**, *31* (2), 527−530.
(96) Laitar, D. S.; Müller, P.; Sadighi, J. P. Efficient Homogeneous Catalysis in the Reduction of CO2 to CO. *J. Am. Chem. Soc.* **2005**, *127* (49), 17196−17197.
(97) Hernán-Gómez, A.; Bradley, T. D.; Kennedy, A. R.; Livingstone, Z.; Robertson, S. D.; Hevia, E. Developing Catalytic Applications of Cooperative Bimetallics: Competitive Hydroamination/Trimerization Reactions of Isocyanates Catalysed by Sodium Magnesiates. *Chem. Commun.* **2013**, *49* (77), 8659−8661.
(98) Paul, F.; Moulin, S.; Piechaczyk, O.; Le Floch, P.; Osborn, J. A. Palladium(0)-Catalyzed Trimerization of Arylisocyanates into 1,3,5-Triarylisocyanurates in the Presence of Diimines: A Nonintuitive Mechanism. *J. Am. Chem. Soc.* **2007**, *129* (23), 7294−7304.
(99) Han, Y. S.; Jung, K. Y.; Kim, Y. J.; Baeck, K. K.; Lee, G. M.; Lee, S. W. Reactivities of Zero-Valent Group 10 Complexes toward Organic Isocyanates: Synthesis of Metallacycles Containing Dimeric Isocyanate Units, Isocyanate Cyclotrimerization, and Computational Chemistry. *New J. Chem.* **2019**, *43* (39), 15614−15625.
(100) Bahili, M. A.; Stokes, E. C.; Amesbury, R. C.; Ould, D. M. C.; Christo, B.; Horne, R. J.; Kariuki, B. M.; Stewart, J. A.; Taylor, R. L.; Williams, P. A.; et al. Aluminium-Catalysed Isocyanate Trimerization, Enhanced by Exploiting a Dynamic Coordination Sphere. *Chem. Commun.* **2019**, *55* (53), 7679−7682.
(101) Siebert, M.; Sure, R.; Deglmann, P.; Closs, A. C.; Lucas, F.; Trapp, O. Mechanistic Investigation into the Acetate-Initiated Catalytic Trimerization of Aliphatic Isocyanates: A Bicyclic Ride. *J. Org. Chem.* **2020**, *85* (13), 8553−8562.
(102) Wang, H. M.; Li, H. X.; Yu, X. Y.; Ren, Z. G.; Lang, J. P. Cyclodimerization and Cyclotrimerization of Isocyanates Promoted by One Praseodymium Benzenethiolate Complex [Pr(SPh)3(THF)-3]. *Tetrahedron* **2011**, *67* (8), 1530−1535.
(103) Zhu, X.; Fan, J.; Wu, Y.; Wang, S.; Zhang, L.; Yang, G.; Wei, Y.; Yin, C.; Zhu, H.; Wu, S.; et al. Synthesis, Characterization, Selective Catalytic Activity, and Reactivity of Rare Earth Metal Amides with Different Metal-Nitrogen Bonds. *Organometallics* **2009**, *28* (13), 3882−3888.
(104) Li, H. X.; Cheng, M. L.; Wang, H. M.; Yang, X. J.; Ren, Z. G.; Lang, J. P. Lanthanide(III) 4,6-Dimethylpyrimidine-2-Thionate Complexes as Efficient Catalysts for Isocyanate Cyclodimerization. *Organometallics* **2011**, *30* (2), 208−214.
(105) Peterson, T. H.; Golden, J. T.; Bergman, R. G. Deprotonation of the Transition Metal Hydride (H5-C5Me5)(PMe3)IrH2. Synthesis and Chemistry of the Strongly Basic Lithium Iridate (H5-C5Me5)-(PMe3)Ir(H)(Li). *Organometallics* **1999**, *18* (10), 2005−2020.
(106) Miranda-Soto, V.; Grotjahn, D. B.; DiPasquale, A. G.; Rheingold, A. L. Imidazol-2-Yl Complexes of Cp*Ir as Bifunctional Ambident Reactants. *J. Am. Chem. Soc.* **2008**, *130* (40), 13200−13201.
(107) Whited, M. T.; Grubbs, R. H. Elucidation of Heterocumulene Activation by a Nucleophilic-at-Metal Iridium(I) Carbene. *Organometallics* **2009**, *28* (1), 161−166.
(108) Pearson, R. G.; Figdore, P. E. Relative Reactivities of Methyl Iodide and Methyl Tosylate with Transition-Metal Nucleophiles. *J. Am. Chem. Soc.* **1980**, *102* (5), 1541−1547.
(109) Grajeda, J.; Kita, M. R.; Gregor, L. C.; White, P. S.; Miller, A. J. M. Diverse Cation-Promoted Reactivity of Iridium Carbonyl Pincer-Crown Ether Complexes. *Organometallics* **2016**, *35* (3), 306−316.
(110) Sciarone, T. J. J.; Nijhuis, C. A.; Meetsma, A.; Hessen, B. Synthesis and Reactivity of Mono(Amidinate) Organoiron(Ii) Complexes. *Dalton Trans.* **2006**, No. 41, 4896−4904.

https://doi.org/10.1021/jacs.1c01725
J. Am. Chem. Soc. XXXX, XXX, XXX−XXX